Structured Distributions of Gas and Solids in Protoplanetary Disks: Theoretical Perspectives

Jaehan Bae (University of Florida)

Structured Distributions of Gas and Solids in Protoplanetary Disks

Jaehan Bae
University of Florida
Carnegie Institution for Science

Andrea Isella
Rice University

Rebecca Martin
University of Nevada, Las Vegas

Satoshi Okuzumi
Tokyo Institute of Technology

Scott Suriano
The University of Tokyo

Zhaohuan Zhu
University of Nevada, Las Vegas

Disk substructure

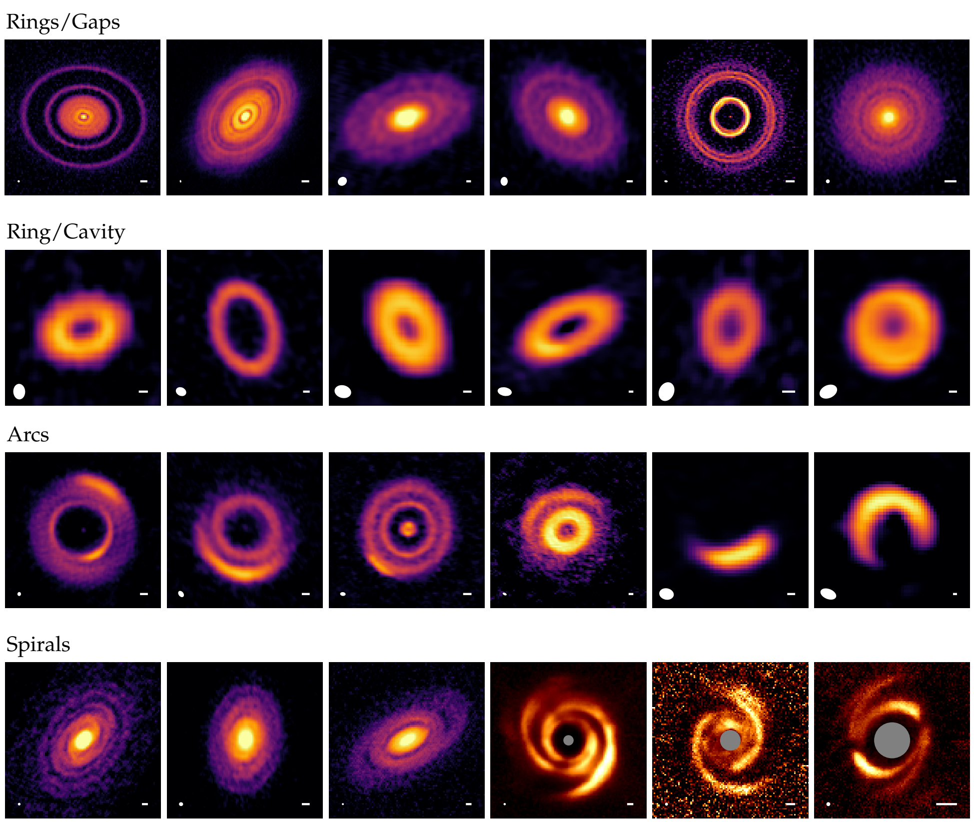

Andrews (2020)

other examples:

velocity kinks, misalignments,

shadows, streamers, clumps, …

In this talk, I will

- focus on spirals and rings/gaps;
- present properties of the observed substructures from a statistical point of view;
- summarize proposed origins of substructures;
- <u>NOT</u> give you answers to what created substructures;
- discuss how we can possibly distinguish different possibilities in the future.

The sample

- Total 423 disks, most of which are located in Taurus, Ophiuchus, Upper Scorpius, Lupus, and Chameleon I star-forming regions.
- Substructures are detected in about 80 disks.

disks with substructures

disks without substructures

◀: upper limit (116 disks)

*The figures show ALMA observations exclusively.

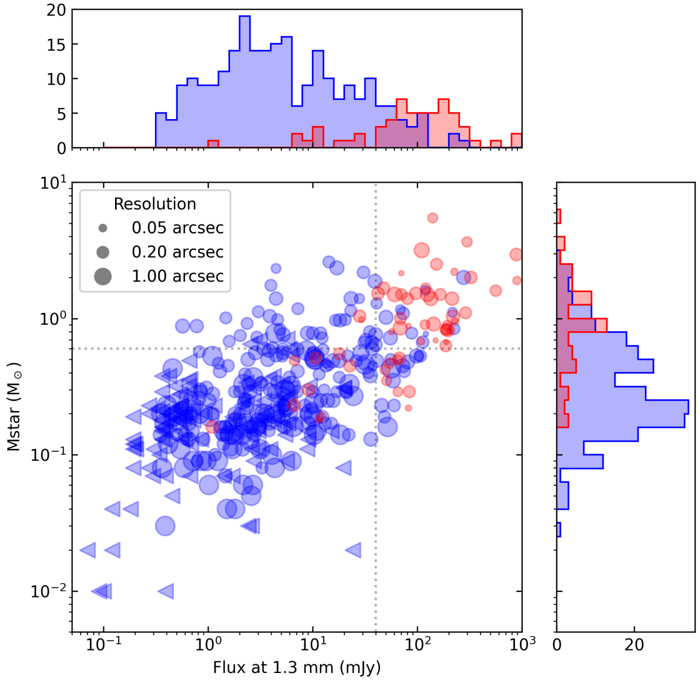

Caveats of the current analysis

- Observational biases DO exist.
  - Brighter disks are observed at higher angular resolution.
- Uncertainties in the disk mass
  - 1.3 mm flux is used to infer the disk mass. For those without 1.3 mm continuum observations, we estimate 1.3 mm flux from 0.87 mm continuum observations.
- Methods to measure the properties of substructures (e.g., width of rings, pitch angle of spirals) differ among literature.
- Limited to nearby low-mass star forming regions.

Caveats of the current analysis

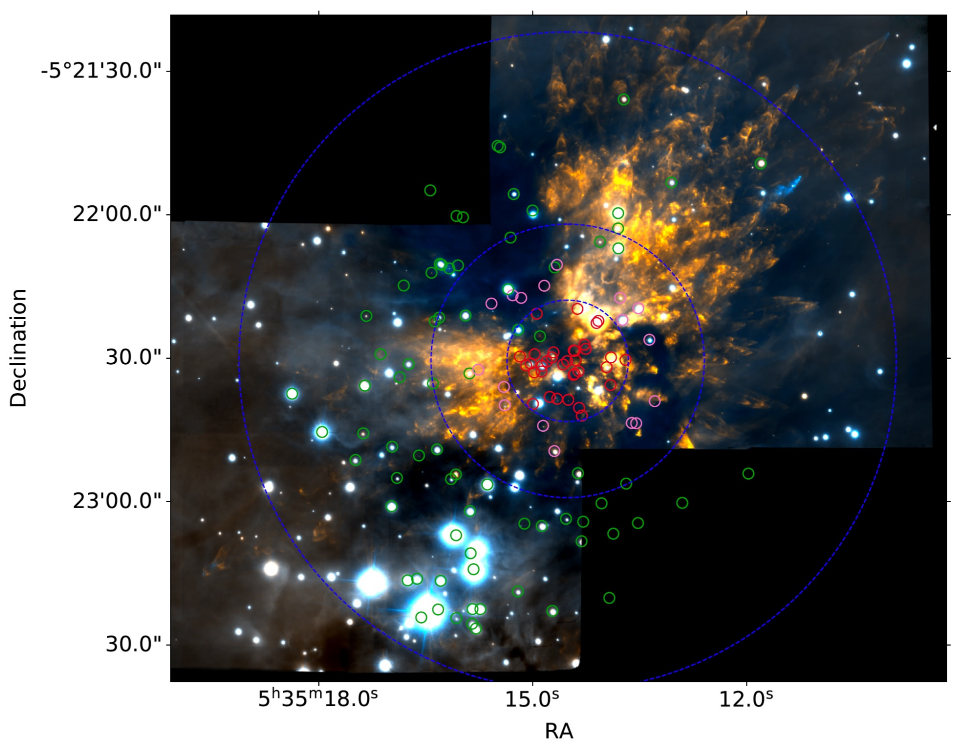

Otter et al. (arXiv:2109.14592, accepted to ApJ)

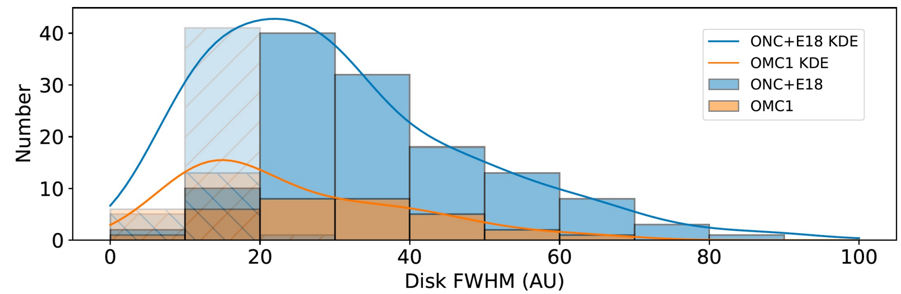

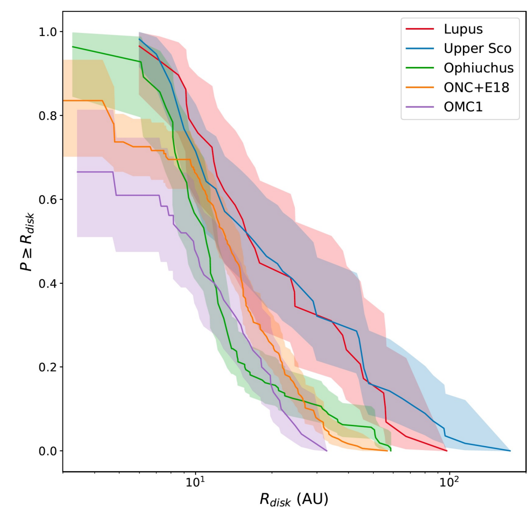

Spirals: potential origins

- companion
- stellar flyby
- gravitational instability
- magneto-hydrodynamic turbulence
- infall

	# of spirals	pitch angle	pattern speed	time variation
companion (Lindblad)				
companion (buoyancy)				
stellar flyby				
GI				
MHD turbulence				
infall				

Spirals: observational data

TABLE 3
SYSTEMS WITH SPIRALS

2MASS Name	Alt. Name	d (pc)	$M_\star$ ($M_\odot$)	$L_\star$ ($L_\odot$)	Class	M_d ($0.01 M_\odot$)	λ	m	ψ ($^\circ$)	radial extent (au)	FWHM (au)	binary sep. ($''$)
J04554582+3033043	ABAur	163	3.17	123.03	II	2.12	mm	2	20	30-90	18	-
							ir	8	22	30-100	10	-
J05302753+2519571	MWC758/HD36112	156	1.5	10.96	II	1.16	mm	2	19	30-80	31	-
							ir	2	19	30-80	4	-
J05355845+2444542	CQTau	162	1.67	10	II	2.31	mm	2	20-40	30-65	19	-
							ir	2	4, 34	30-60	16	-
J03454828+3224118	LkHa330	309	2.95	22.91	II	16.97	ir	2	12-16	60-150	46	-
J04555938+3034015	SUAur	158	2.18	14.45	II	0.58	ir	6	-	-	11	-
J05380526-0115216	V1247Ori	398	1.9	15.81	PTD	7.72	ir	1	6.5	96-119	16	-
J04300399+1813493	UXTauA	140	1.67	3.24	TD	0.91	mm	2	20-30	140-280	18	2.7
							ir	2	-	-	18	2.7
J05194140+0538428	HD34700A	356	4.1	25.12	II	0.8	ir	6	27-55	110-320	18	5.2
J16264502-2423077	GSS39/Elias2-27	116	0.63	1.51	II	3.59	mm	2	16	47-244	6	-
J16484562-1416359	WaOph6	123	0.68	2.88	II	2.08	mm	2	14 9-18	20-70	7	-
							ir	2	14-20	20-45	7	-
-	SR21	138	2.5	12.59	II	2.93	ir	2	2-14	25-40	7	-
J11100010-7634578	WWCha	192	1.9	2.69	II	17.18	ir	1	-	-	13	-
J11332542-7011412	HD100546	110	2.2	25.12	TD	4.34	ir	6	-	-	6	-
J11493184-7851011	DZCha	110	0.5	1	-	0.07	ir	2	27	5-25	6	-
J11015191-3442170	TWHya	60	0.8	0.28	II	1.72	mm	3	3-9	70-210	1	-
J15560921-3756057	Sz82,IMLup	158	0.95	2.57	II	4.37	mm	2	10-22	30-94	8	-
J15564230-3749154	Sz83,RULup	160	0.67	1.48	II	3.65	ir	5	21-31	250-1200	4	-
J15451286-3417305	Sz68,HTLup	154	2.15	5.37	II	1.35	mm	2	17	13-39	4	2.8
J15564188-4219232	HD142527	157	2.1	16.22	II/TD	24.85	mm	3	3-17	290-670	31	0.1
							ir	6	-	80-130	31	0.1
J11330559-5419285	HD100453	103	1.5	10	-	1.35	mm	2	6	20-30	3	1.045
						1.35	ir	2	14-18	20-30	3	1.045
J15154844-3709160	SAO206462/HD135344B	135	1.6	9.77	TD	10.79	ir	2	11	38-107	12	-
J16113134-1838259	AS205N	128	0.99	2.19	-	12.65	mm	2	14	19-68	6	1.3

Spirals: statistics

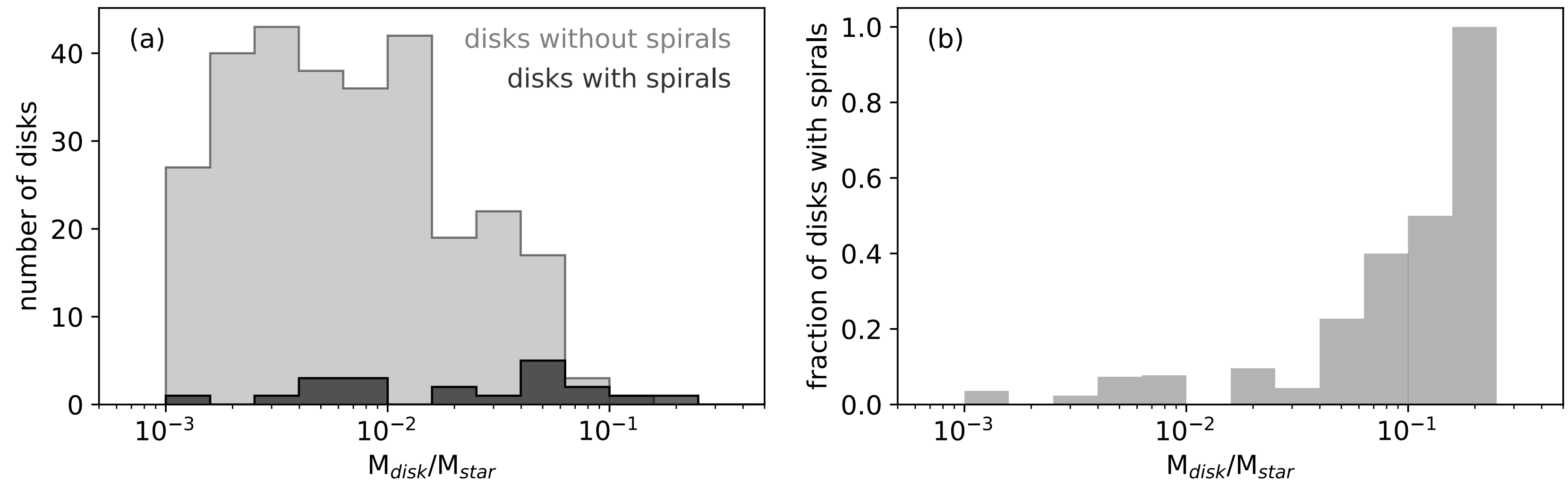

- Spirals are detected in a larger fraction of massive disks ($M_{disk}/M_{star} \gtrsim 0.04$) compared with the low-mass counterpart.

Spirals: statistics

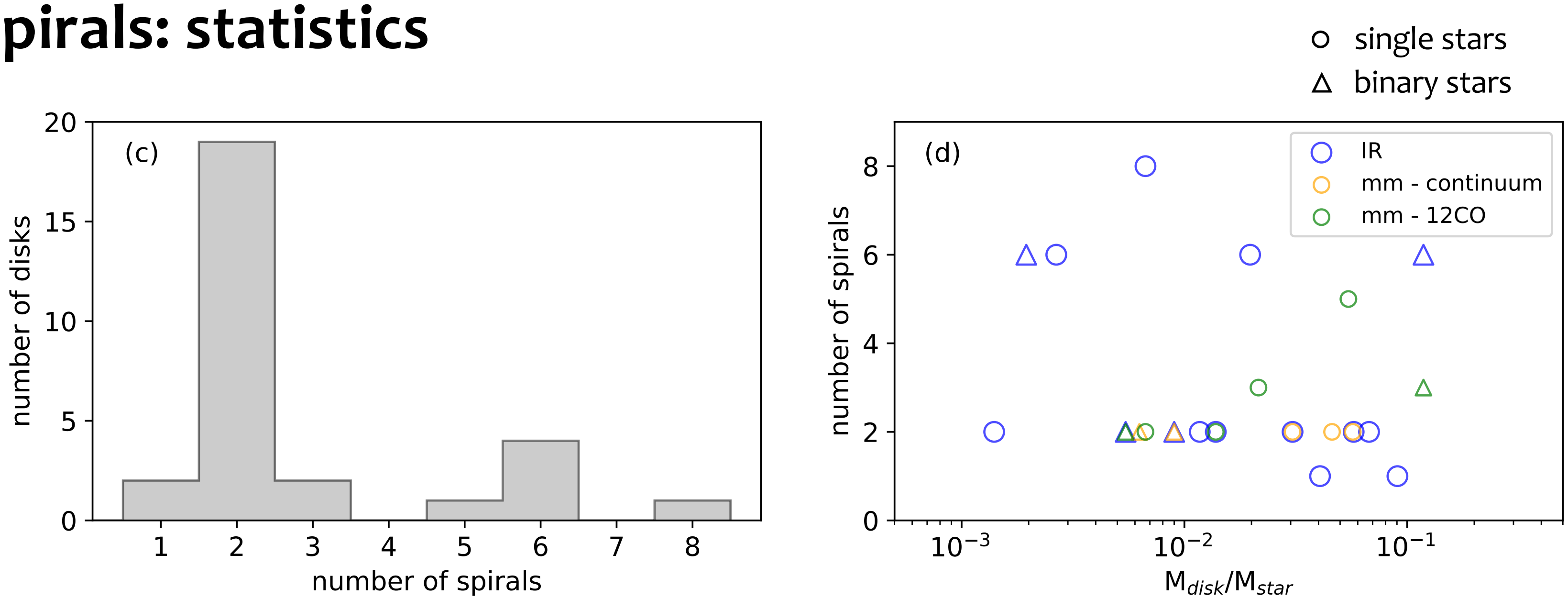

- m=2 spirals are dominant (19/29).
- No clear trend is found between the number of spirals and M_{disk}/M_{star}.
- In mm continuum, only two-armed spirals are found until now.

Spirals: statistics

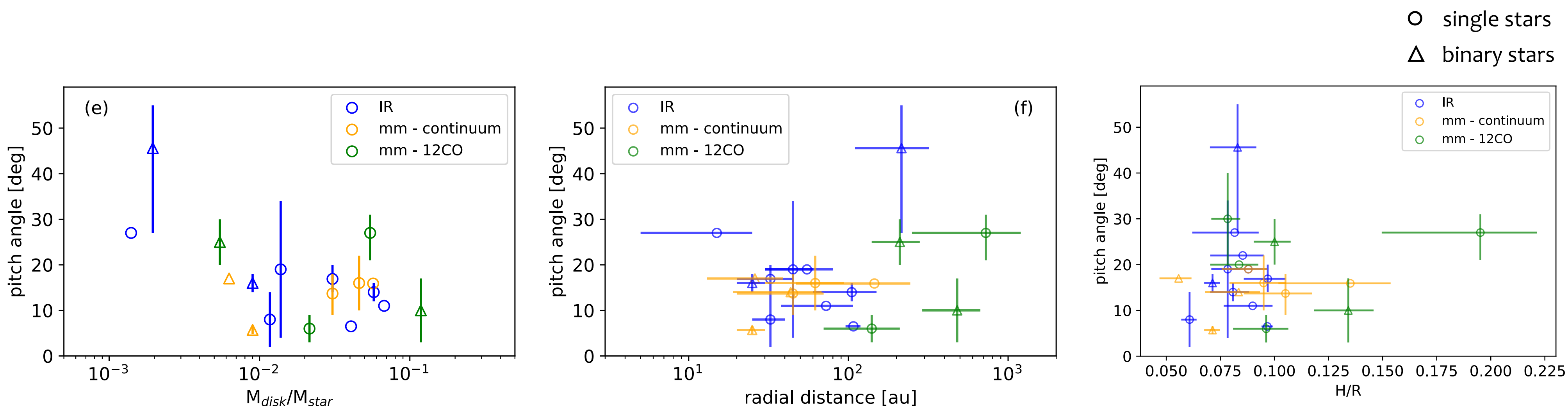

- Pitch angle might decrease as a function of M_{disk}/M_{star}.
- There is a weak trend that the pitch angle increases as a function of the radial location of the spirals, H/R, or sound speed.

Spirals by a companion – Lindblad resonances

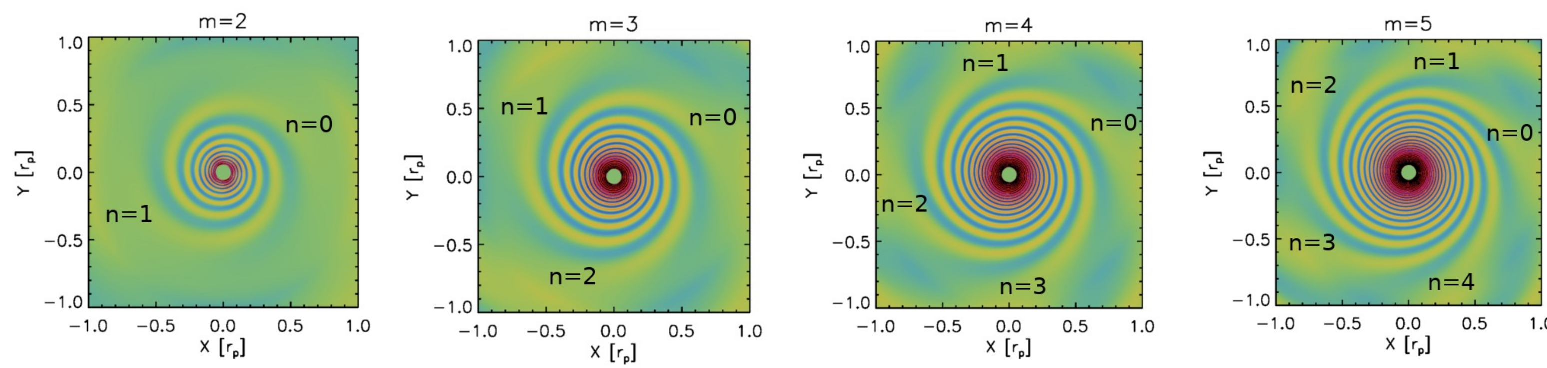

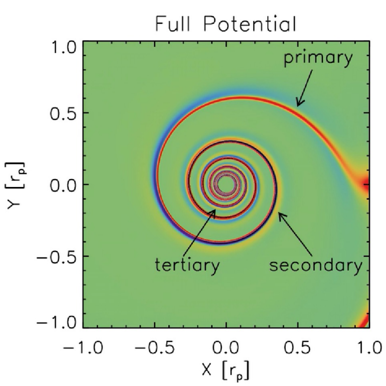

<u>Constructive interference</u> between different azimuthal modes forms spirals.

$$\phi_m(r) = \phi_m(r_0) - \int_{r_0}^{r} \frac{\Omega(r')}{c_s(r')} \left| \left(1 - \frac{r'^{3/2}}{r_p^{3/2}}\right)^2 - \frac{1}{m^2} \right|^{1/2} \mathrm{d}r'$$

Bae & Zhu (2018a,b), see also Miranda & Rafikov 2019

Spirals by a companion – Lindblad resonances

- A smaller number of spirals are excited for more massive companions.
  - Stronger waves propagate faster.

$M_{th} = (h/r)_p^3 M_*$

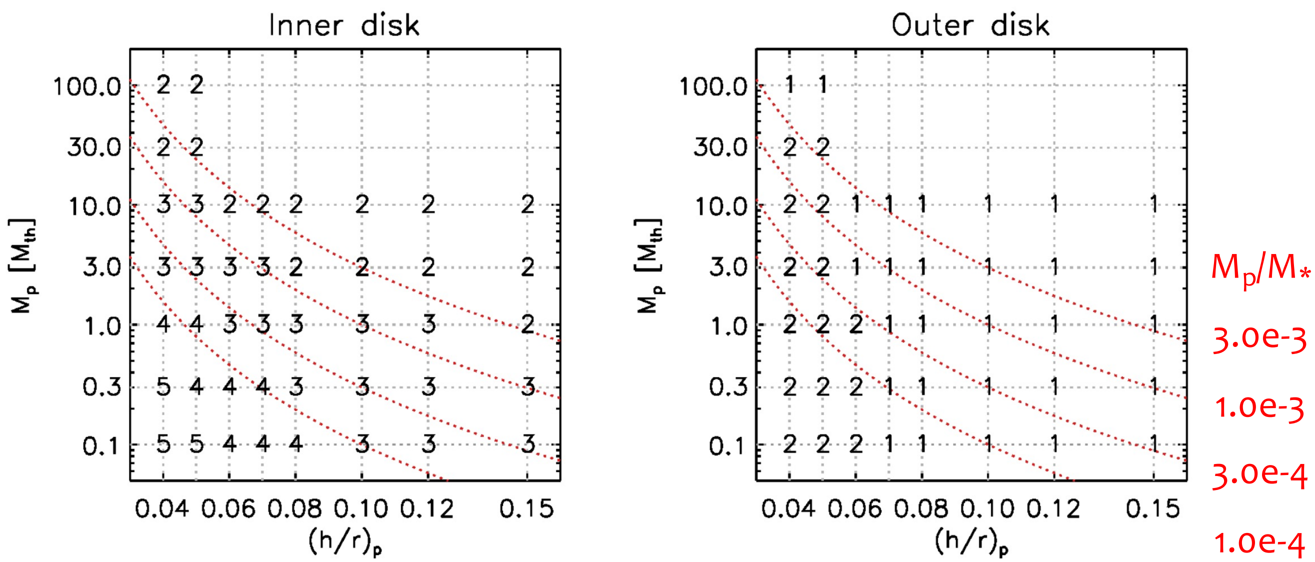

Bae & Zhu (2018a,b)

Spirals by a companion – Lindblad resonances

- Additional second-order spirals excite for companions having non-zero orbital eccentricity.

$$\phi^s_{m,m} = -\frac{GM_s}{2a}(2-\delta_{m,0})(b^m_{1/2} - f\beta\delta_{m,1}),$$

$$\phi^s_{m+1,m} = -\frac{GM_s}{2a}e(2-\delta_{m,0})\left[\left(\frac{1}{2}+\frac{m\Omega_s}{\kappa_s}+\frac{\beta}{2}\frac{d}{d\beta}\right)b^m_{1/2} - f\beta\left(\frac{3}{2}-\frac{2B_s}{\Omega_s}+\frac{\Omega_s}{\kappa_s}\right)\delta_{m,1}\right],$$

$$\phi^s_{m-1,m} = -\frac{GM_s}{2a}e(2-\delta_{m,0})\left[\left(\frac{1}{2}-\frac{m\Omega_s}{\kappa_s}+\frac{\beta}{2}\frac{d}{d\beta}\right)b^m_{1/2} - f\beta\left(\frac{3}{2}-\frac{2B_s}{\Omega_s}-\frac{\Omega_s}{\kappa_s}\right)\delta_{m,1}\right].$$

Goldreich & Tremaine (1980)

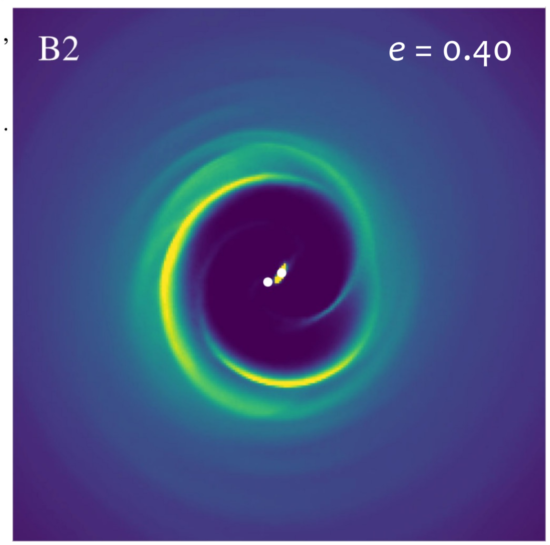

Price et al. (2018)

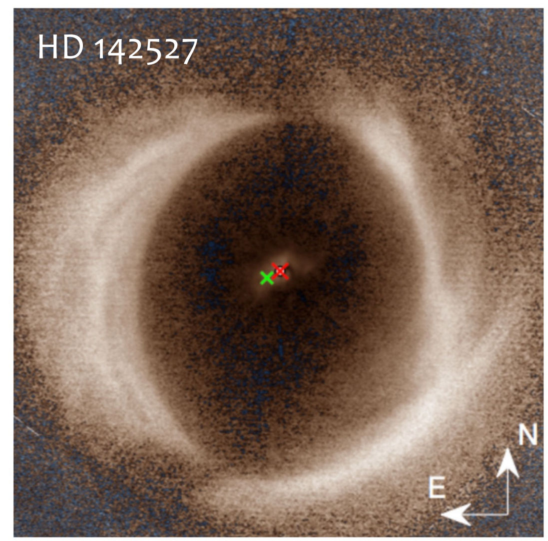

Avenhaus et al. (2017)

Spirals by a companion – Lindblad resonances

- Thermodynamics matters.

Tc = β = cooling timescale/dynamical timescale

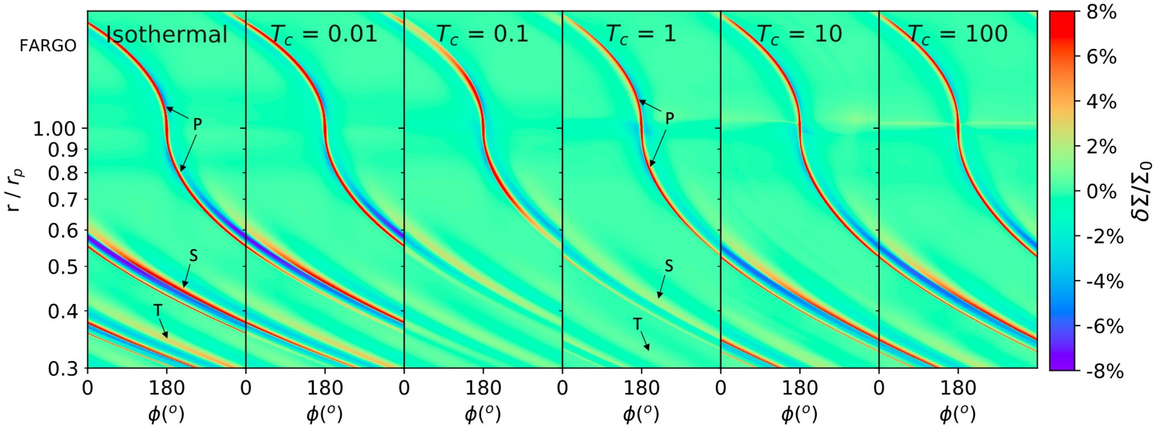

$$l_F^m = \left(\frac{\mathrm{d}\ln F_J^m}{\mathrm{d}r}\right)^{-1}$$

the length scale of the radial variation of the angular momentum flux

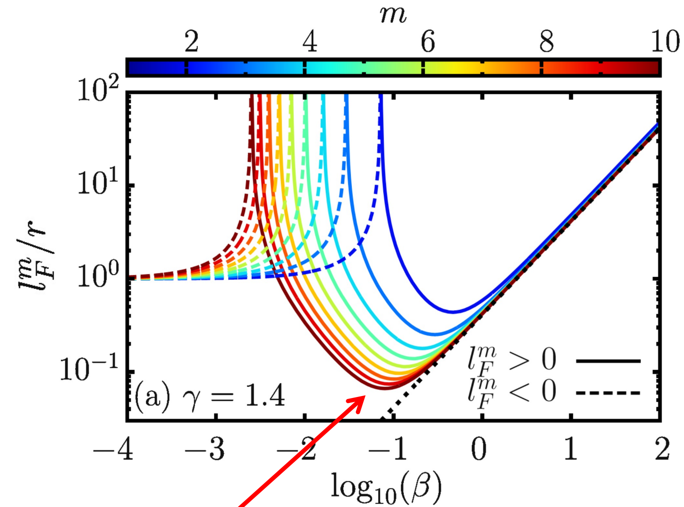

strong linear damping via cooling

left: Zhang & Zhu 2020, right: Miranda & Rafikov 2020

Spirals by a companion – Lindblad resonances

- Pitch angle increases as a function of the companion mass.

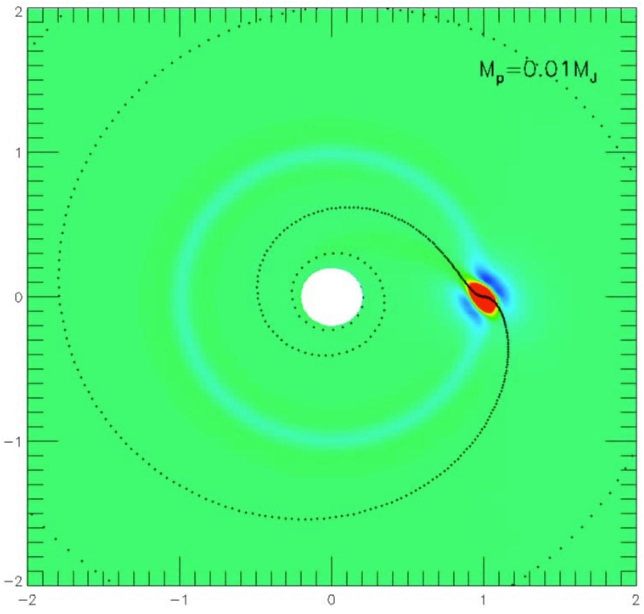

movie credit: Zhaohuan Zhu

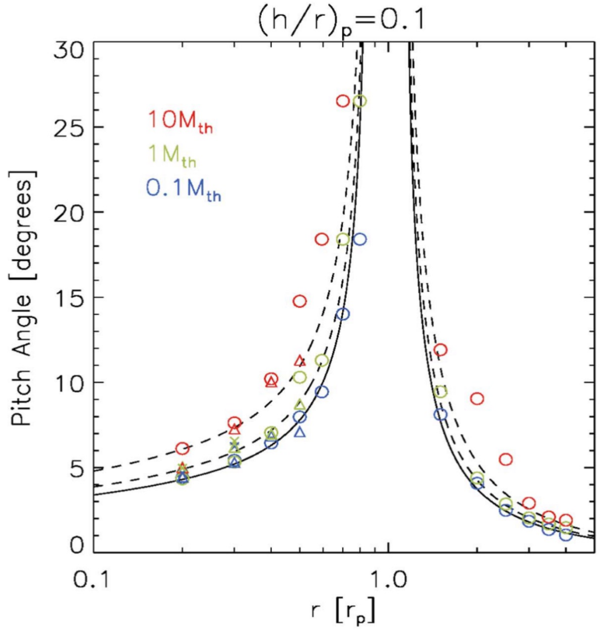

Bae & Zhu (2018b)

Spirals by a companion – Lindblad resonances

- Pitch angle increases as a function of the sound speed.

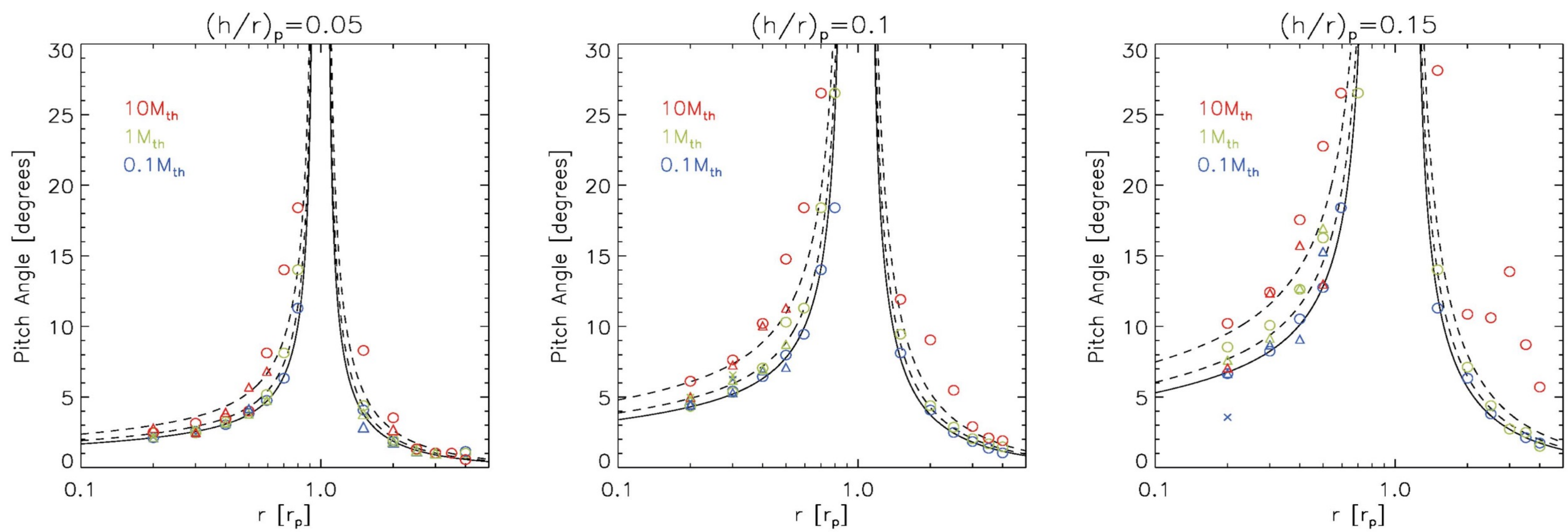

Bae & Zhu (2018b)

Spirals by a companion – Lindblad resonances

- Pitch angle increases as a function of the sound speed.
  - Vertical disk temperature structure matters.

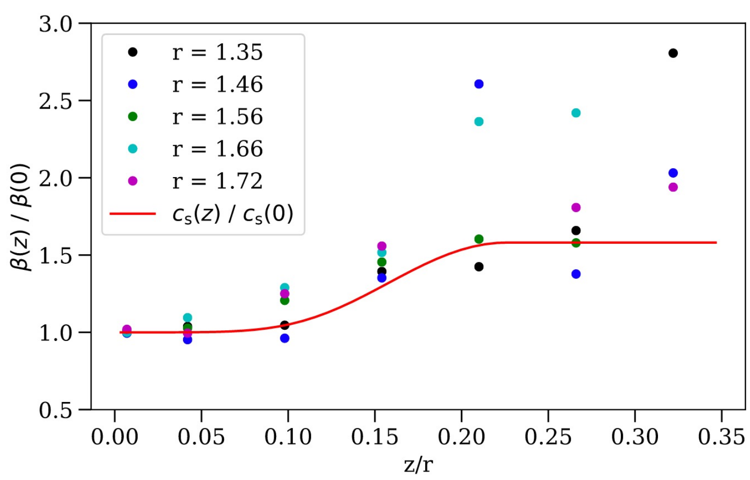

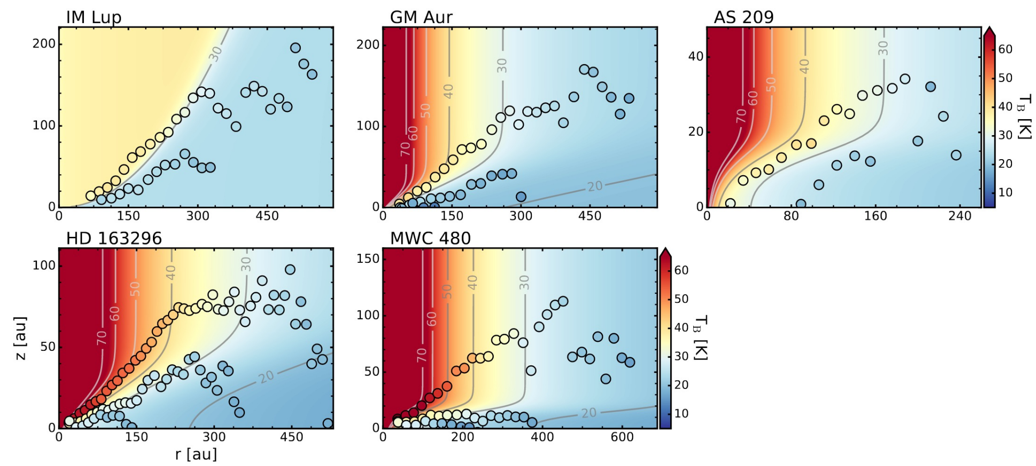

Juhász & Rosotti (2018)

Law et al. (2021), MAPS

Spirals by a companion – Lindblad resonances

- Pitch angle increases as a function of the sound speed.
  - Vertical disk temperature structure matters.

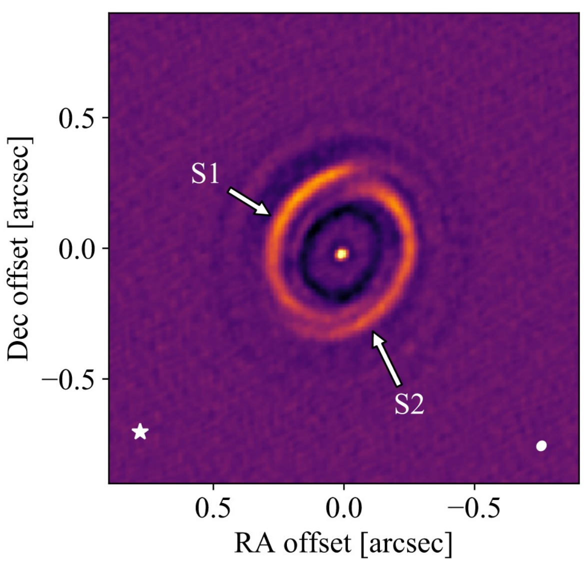

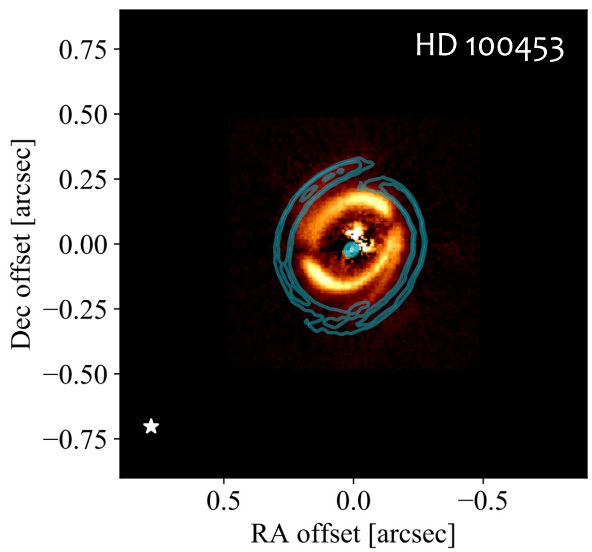

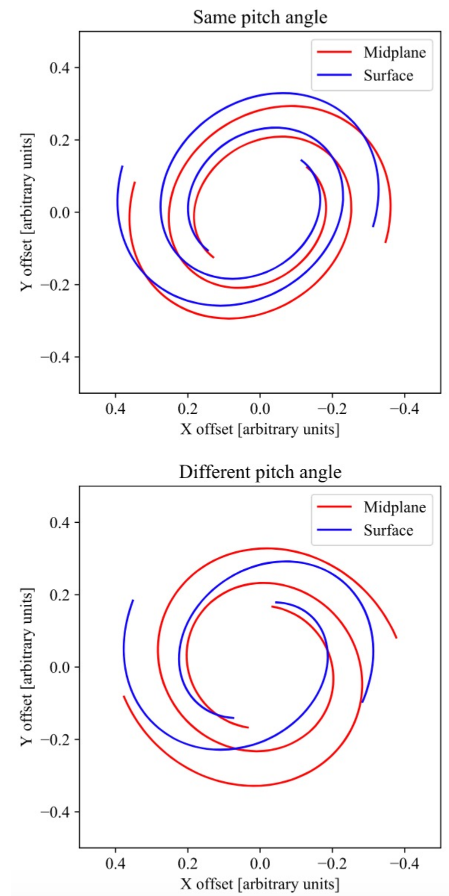

Rosotti et al. (2021)

Spirals by a companion – Lindblad resonances

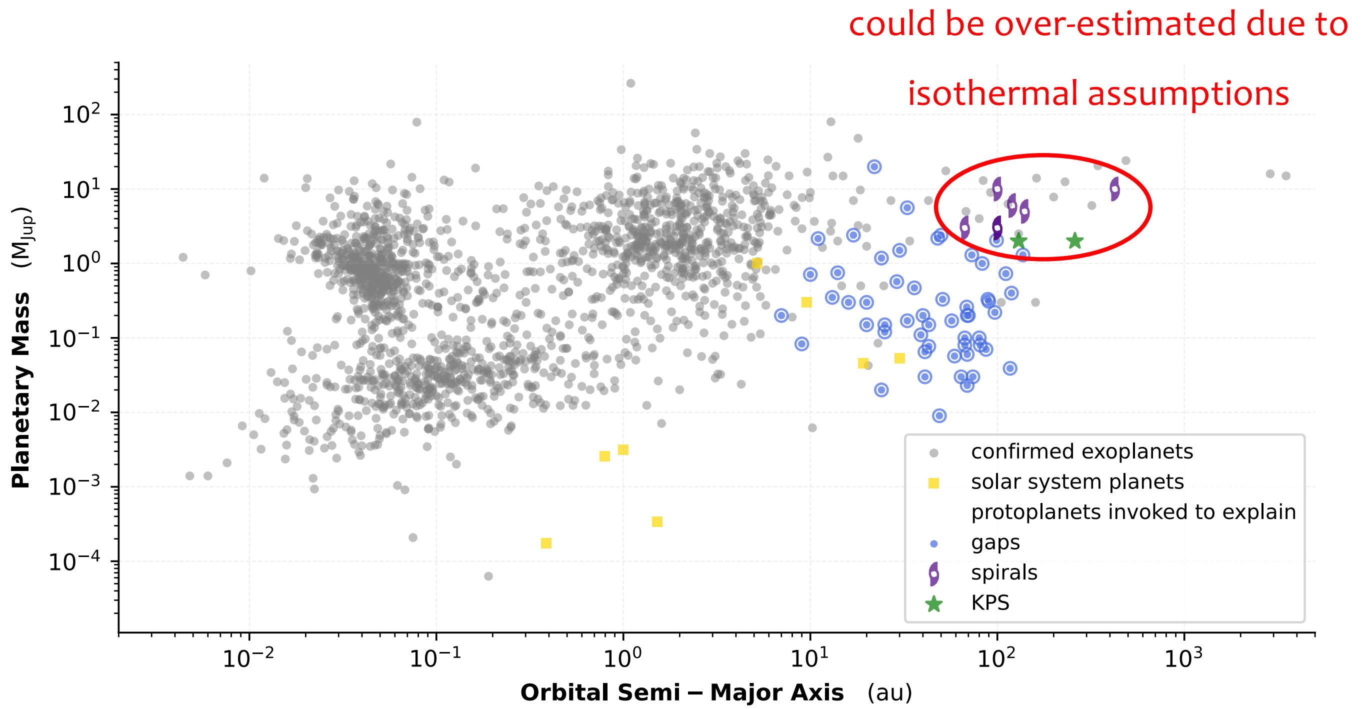

Updated from Bae et al. (2018), Disk Dynamics et al. (2020)

Spirals by a companion – Lindblad resonances

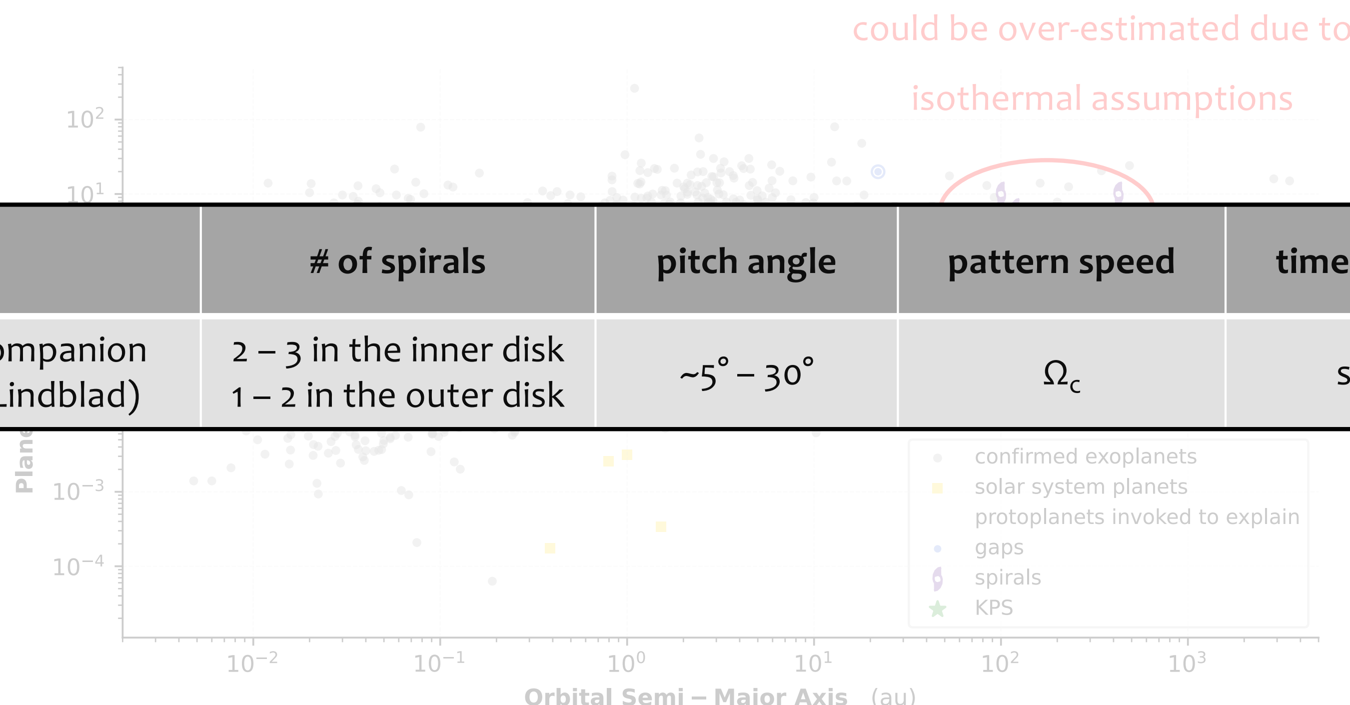

	# of spirals	pitch angle	pattern speed	time variation
companion (Lindblad)	2 – 3 in the inner disk 1 – 2 in the outer disk	~5° – 30°	Ω_c	steady

Updated from Bae et al. (2018), Disk Dynamics et al. (2020)

Spirals by a companion – buoyancy resonances

N: buoyancy frequency (a.k.a. Brunt-Väisälä frequency)

$$N^2 = \frac{g}{\gamma}\frac{\partial}{\partial z}\left[\ln\left(\frac{P}{\rho^\gamma}\right)\right]$$

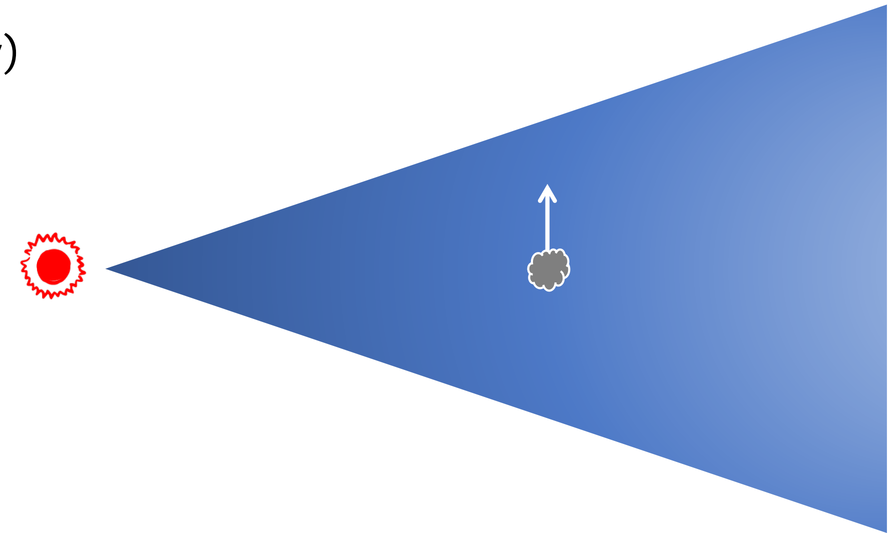

When a gas parcel is vertically displaced,

- if $N^2>0$, the gas parcel will vertically oscillate;
- if $N^2=0$, the gas parcel won't move any further;
- if $N^2<0$, the gas parcel will further rise.

For a vertically isothermal disk with an isothermal EOS, $P = \rho c_s^2$ and $\gamma = 1$. → $N^2=0$

For a vertically stratified disk (hotter surface) with an adiabatic EOS, $N^2>0$

Spirals by a companion – buoyancy resonances

When planet's orbital frequency matches to the buoyancy frequency, the oscillatory motion can amplify through the resonance: buoyancy resonance.

Zhu et al. (2012), Lubow & Zhu (2014)

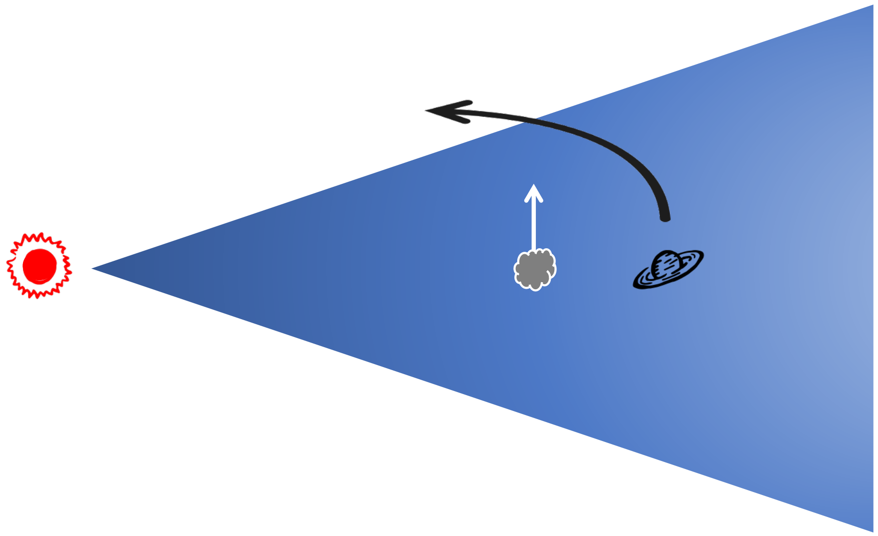

Spirals by a companion – buoyancy resonances

Isothermal

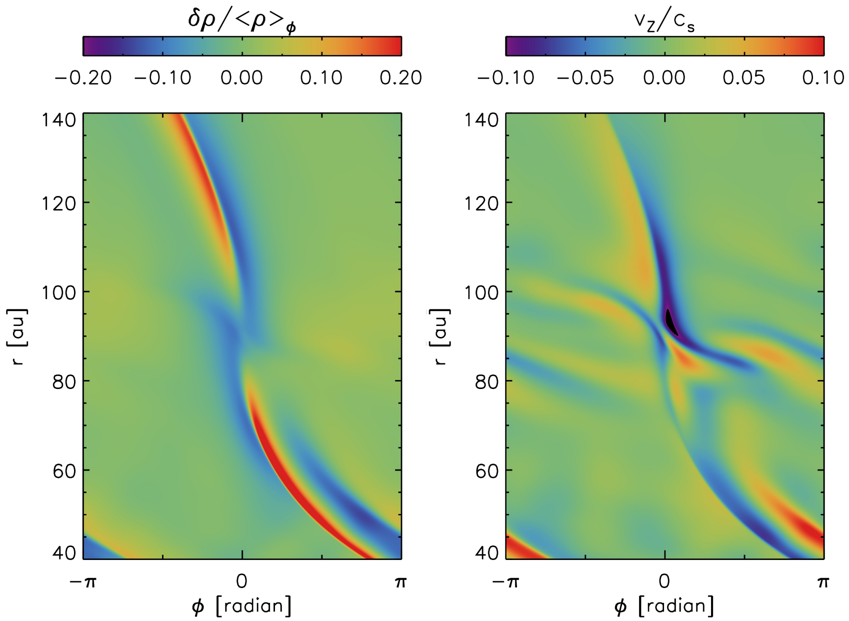

Adiabatic

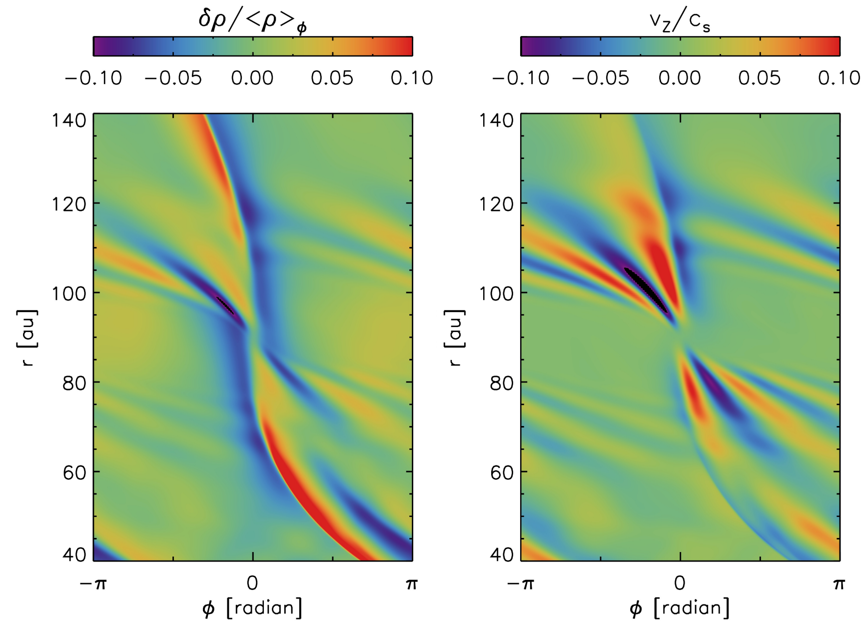

Bae et al. (2021)

Spirals by a companion – buoyancy resonances

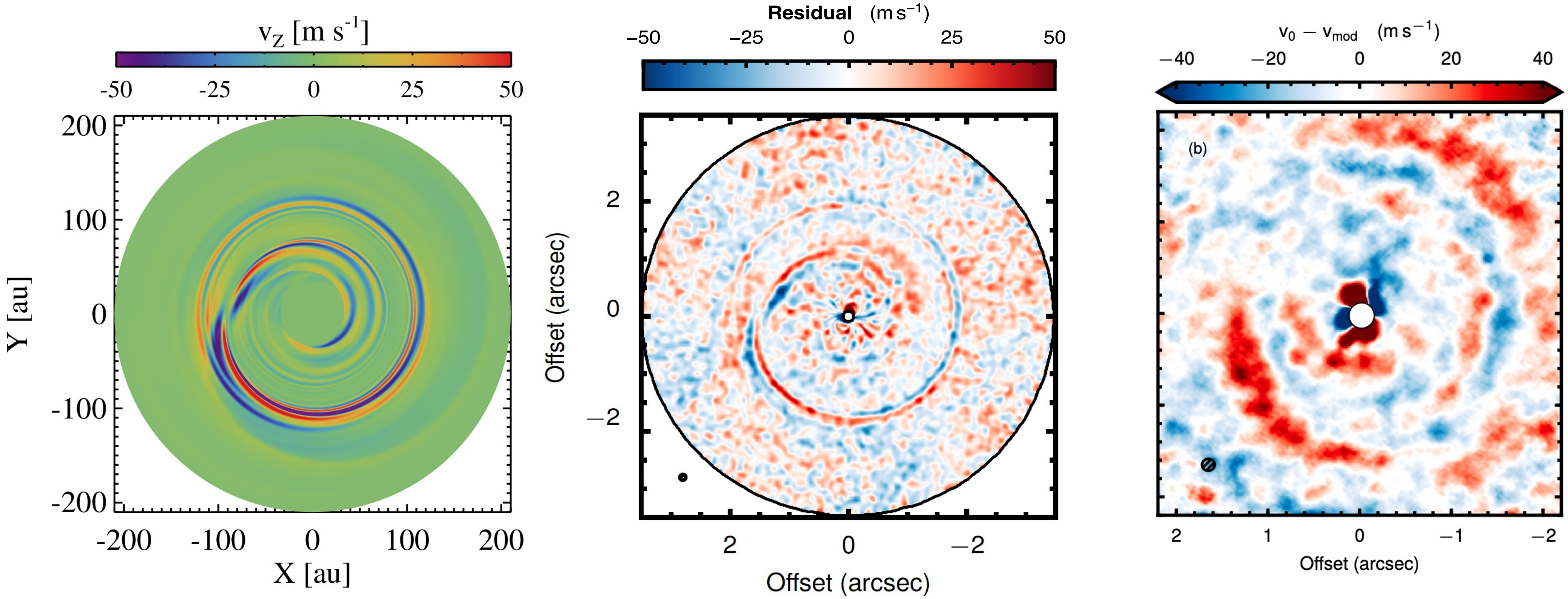

Bae et al. (2021)

Teague, Bae et al. (2019)

Spirals by a companion – buoyancy resonances

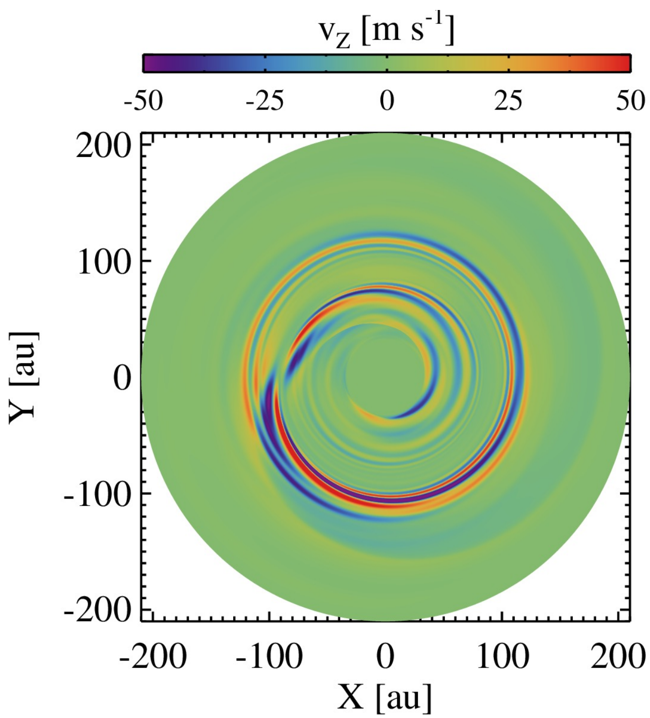

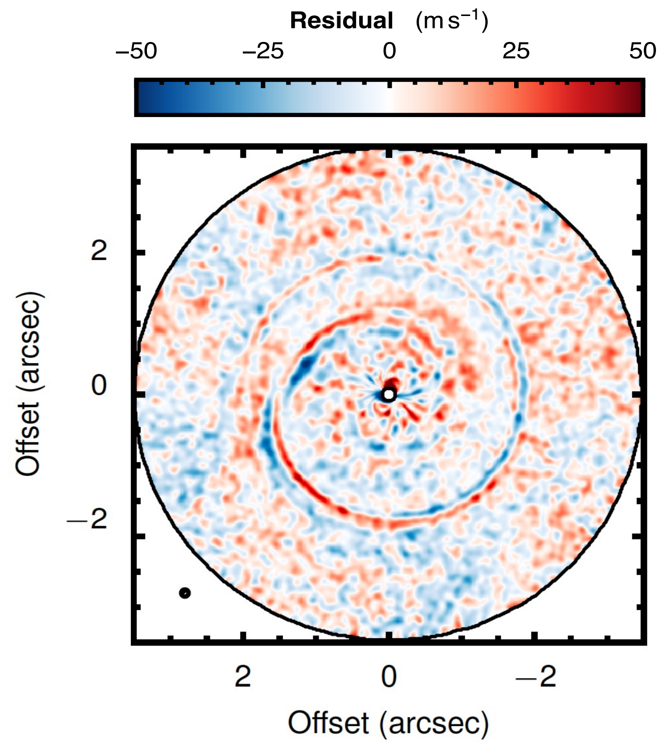

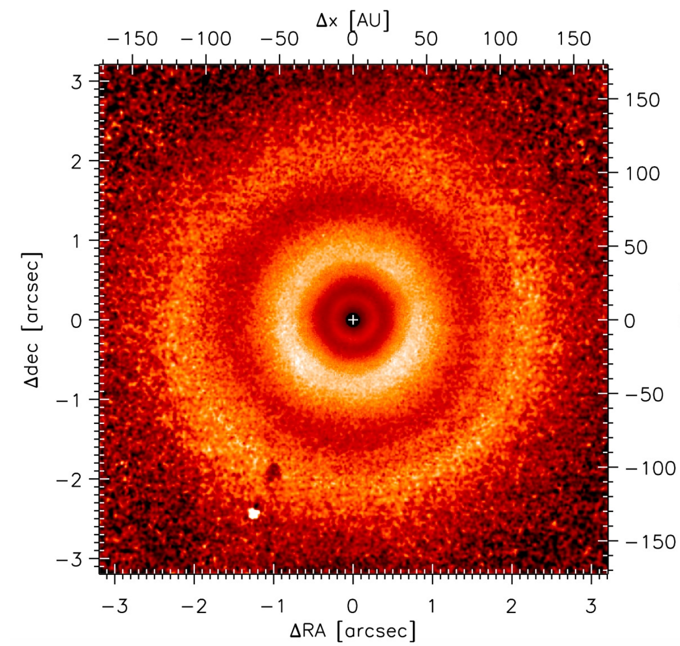

Bae et al. (2021)

van Boekel et al. (2017)

Spirals by a companion – buoyancy resonances

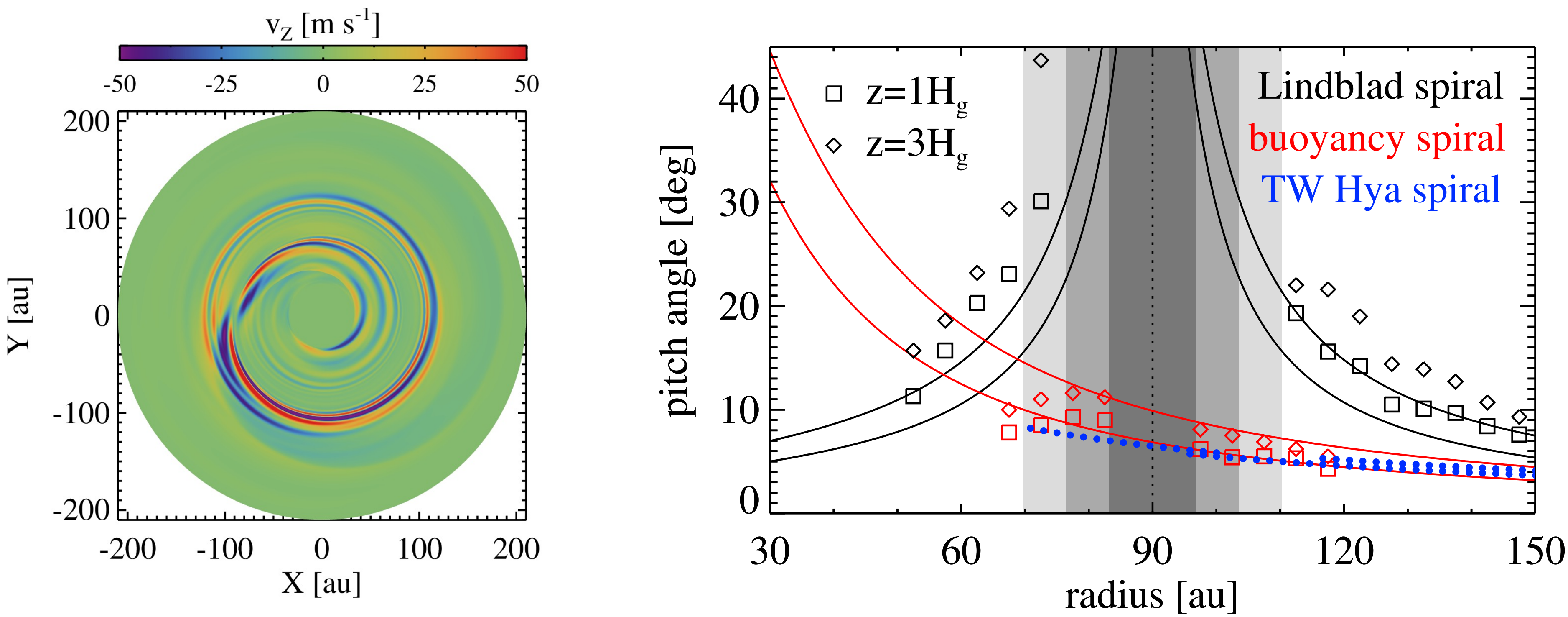

Bae et al. (2021)

Spirals by a companion – buoyancy resonances

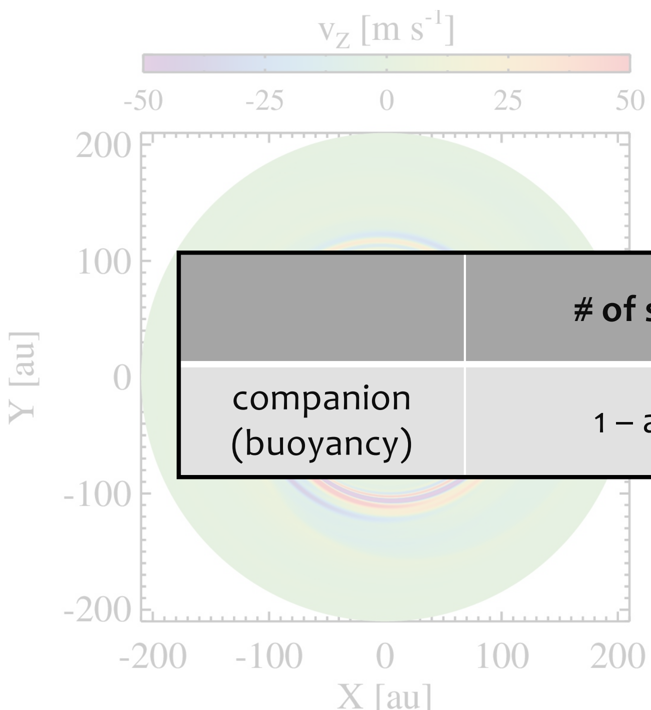

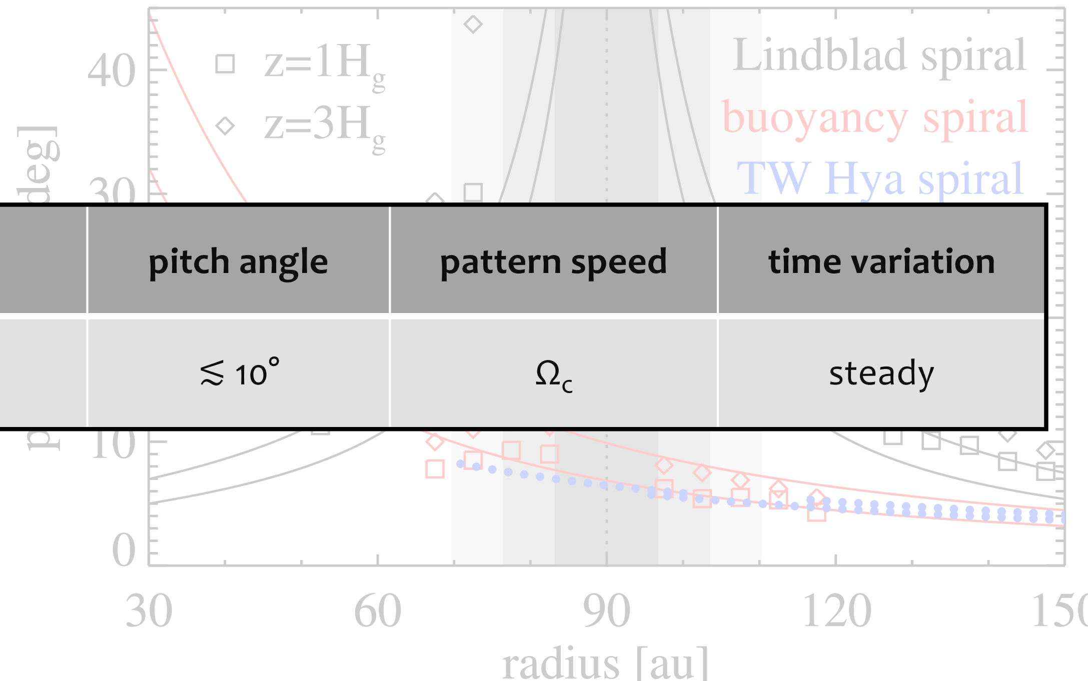

	# of spirals	pitch angle	pattern speed	time variation
companion (buoyancy)	1 – a few	$\lesssim 10^\circ$	Ω_c	steady

Bae et al. (2021)

Spirals by stellar flyby

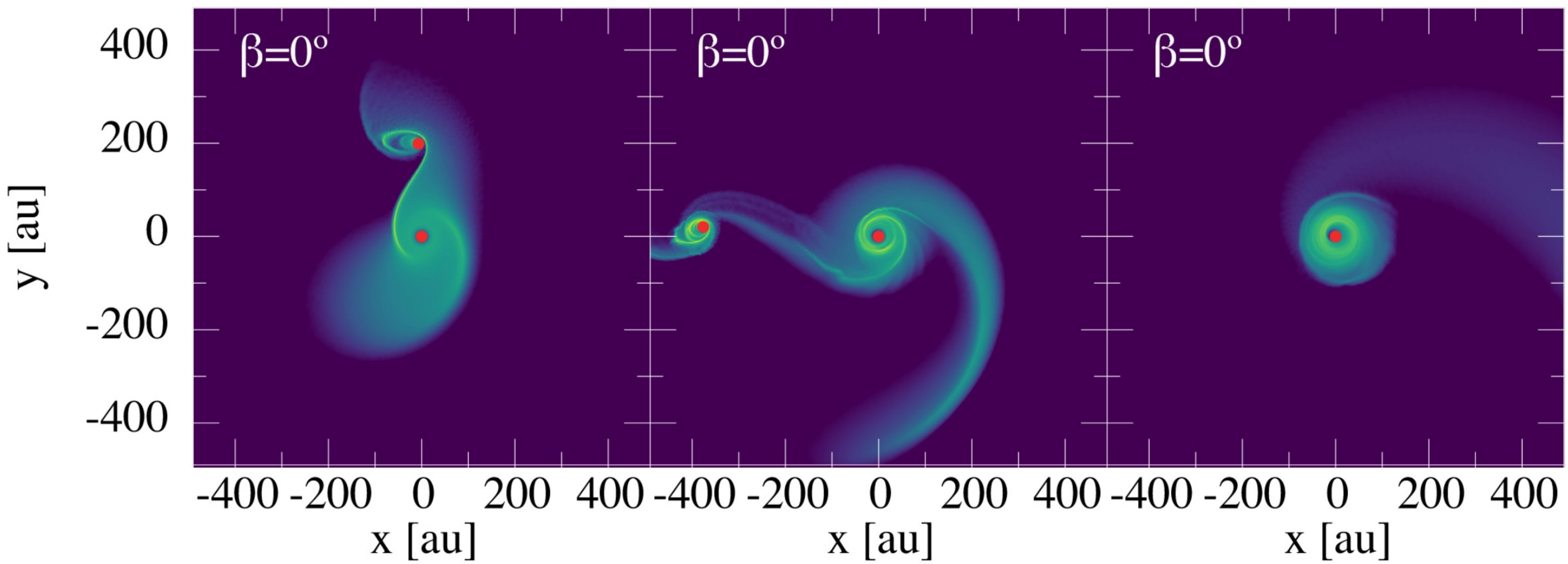

Cuello et al. (2019)

see also Thies et al. (2010), Cuello et al. (2020), Nealon et al. (2020)

Spirals by stellar flyby

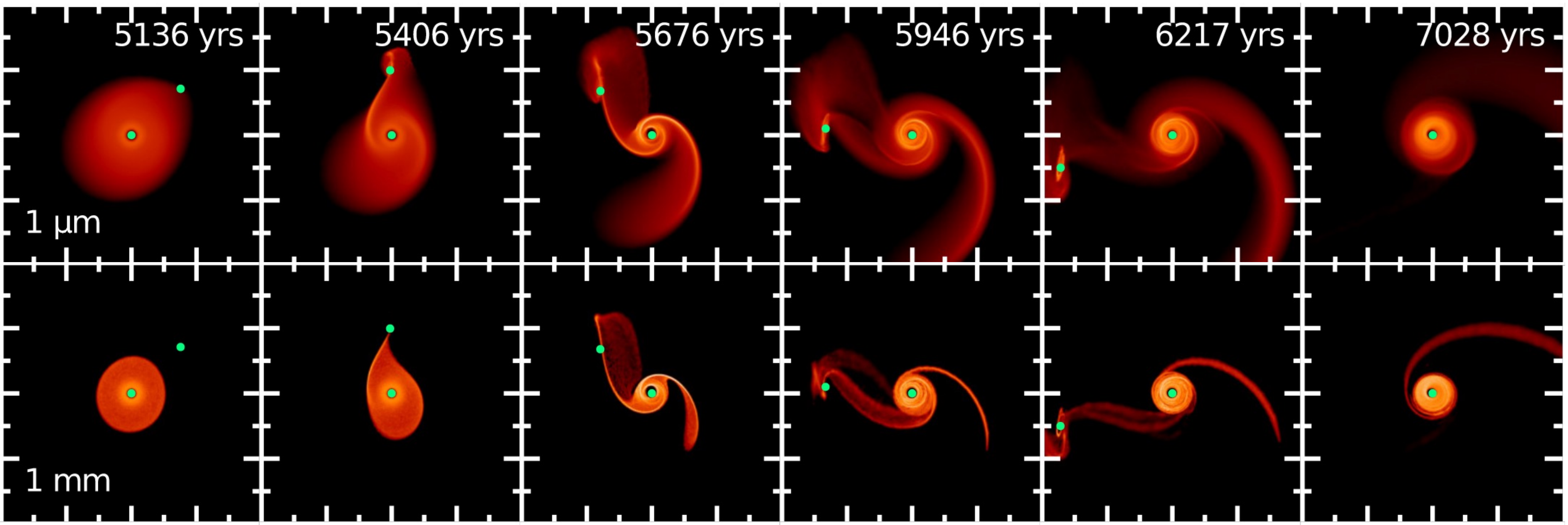

Cuello et al. (2019)

see also Thies et al. (2010), Cuello et al. (2020), Nealon et al. (2020)

Spirals by stellar flyby

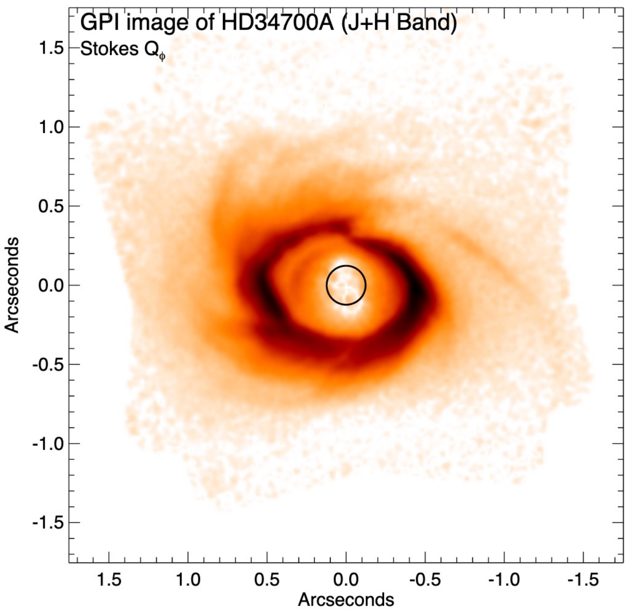

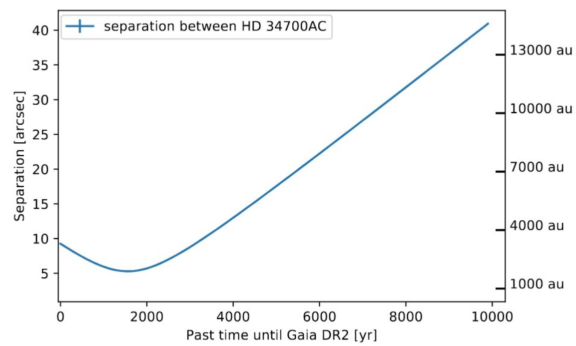

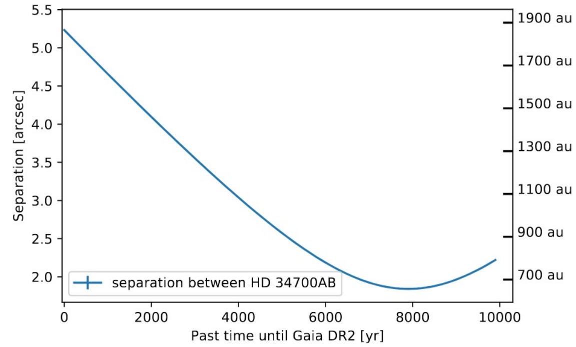

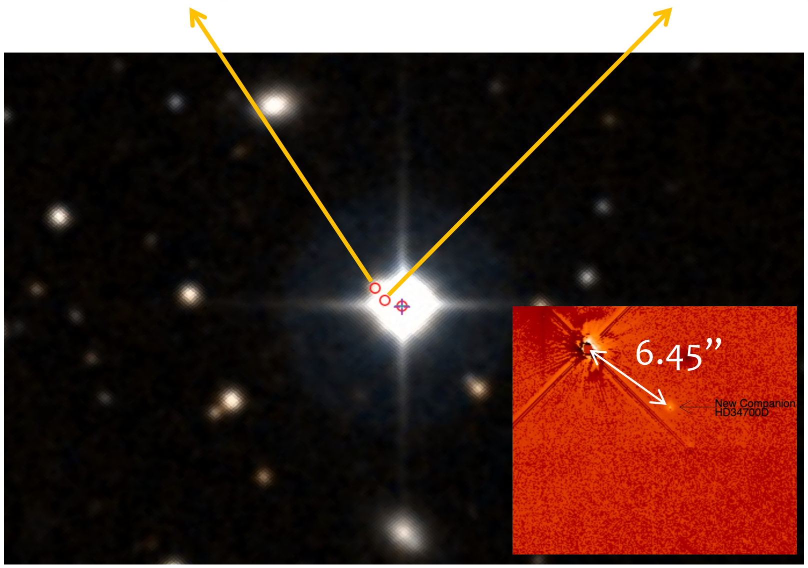

Monnier et al. (2019), Uyama et al. (2020)

Spirals by stellar flyby

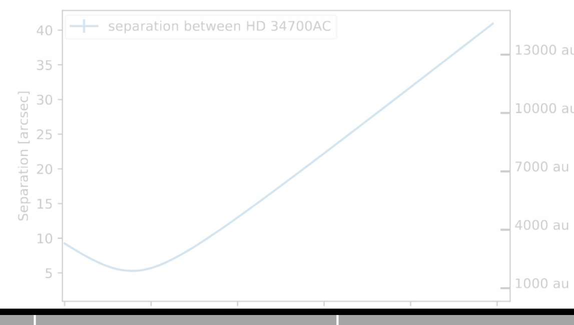

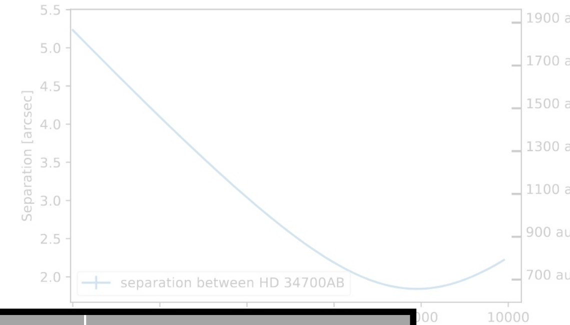

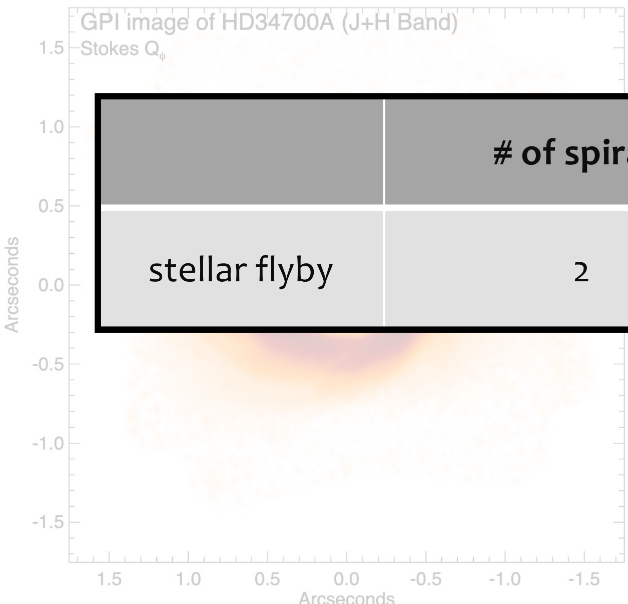

	# of spirals	pitch angle	pattern speed	time variation
stellar flyby	2	~10° – 30°	~Ω_c	disappear on the wave propagation timescale after the encounter

Monnier et al. (2019), Uyama et al. (2020)

Spirals by GI

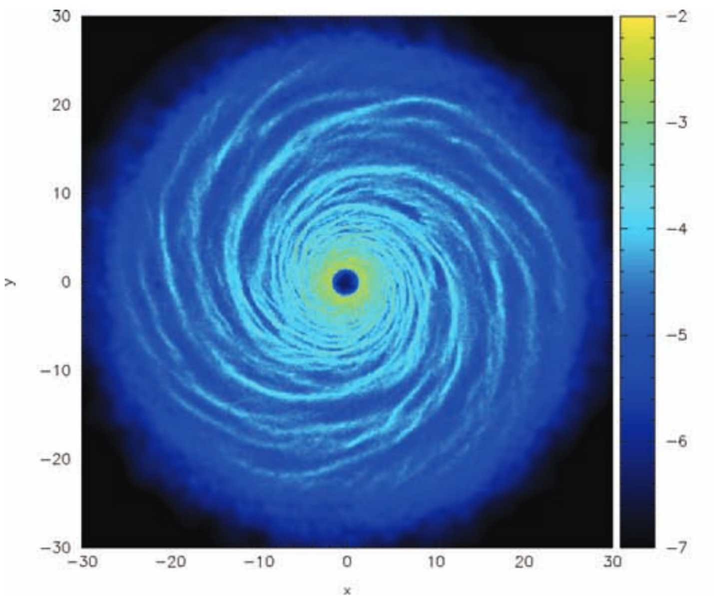

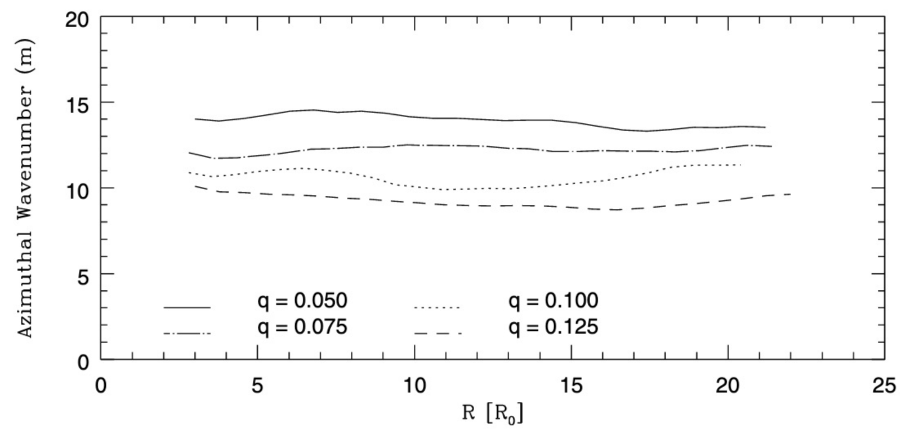

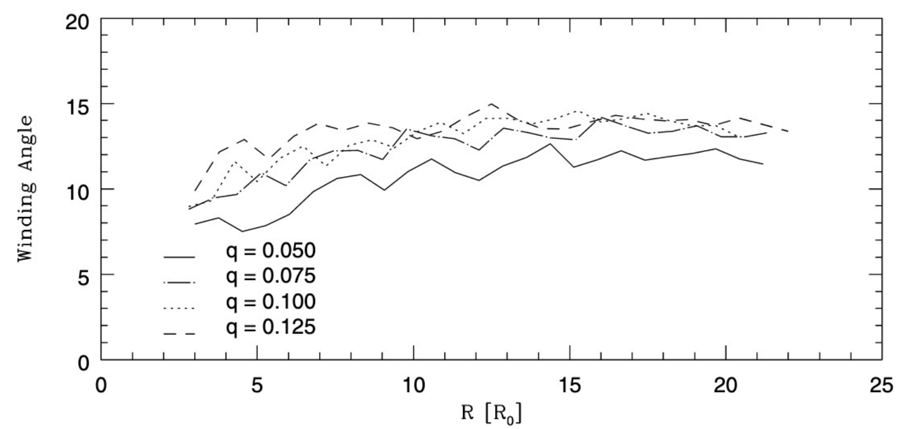

Cossins et al. (2009)

Spirals by GI

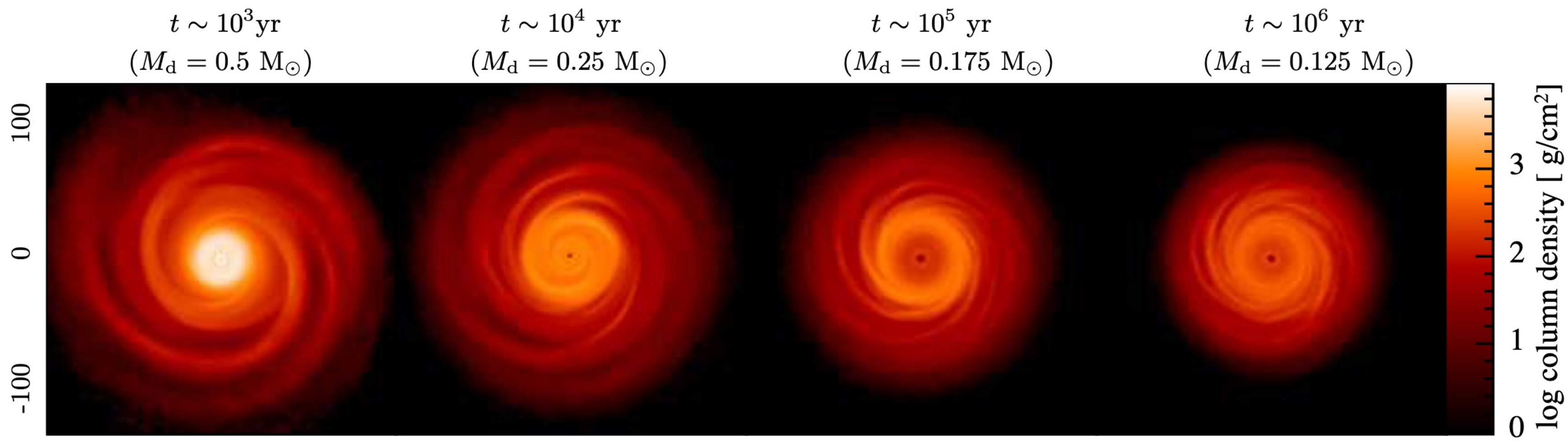

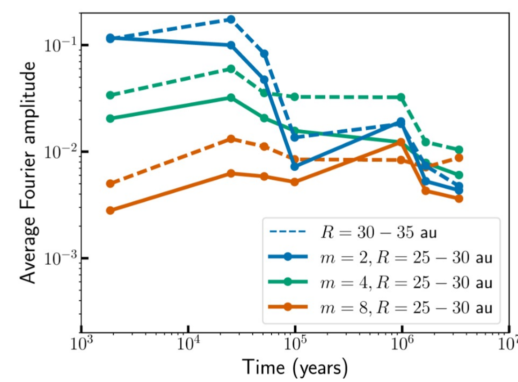

Hall et al. (2019)

see also Forgan et al. (2011), Bethune et al. (2021)

Spirals by GI

	# of spirals	pitch angle	pattern speed	time variation
GI	2 – 10	~5° – 15°	Ω_K	variable

Hall et al. (2019)

see also Forgan et al. (2011), Bethune et al. (2021)

Spirals by MHD turbulence

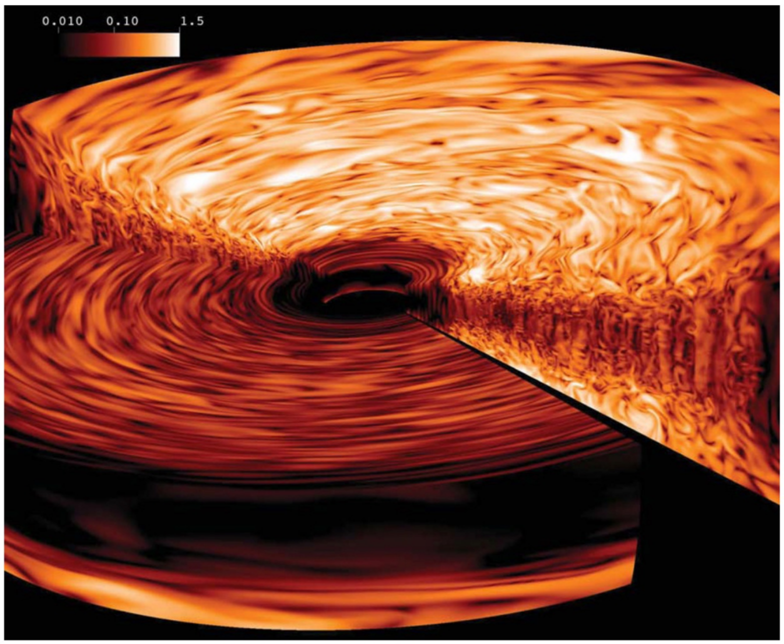

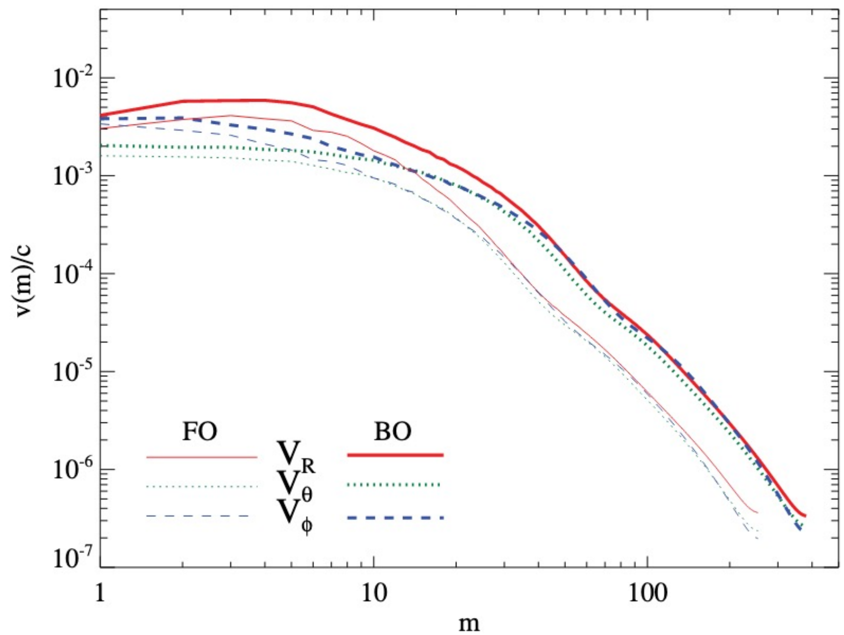

Flock et al. (2011)

see also Heinemann & Papaloizou (2009), Suzuki & Inutsuka (2014), Gogichaishvili et al. (2017)

Spirals by MHD turbulence

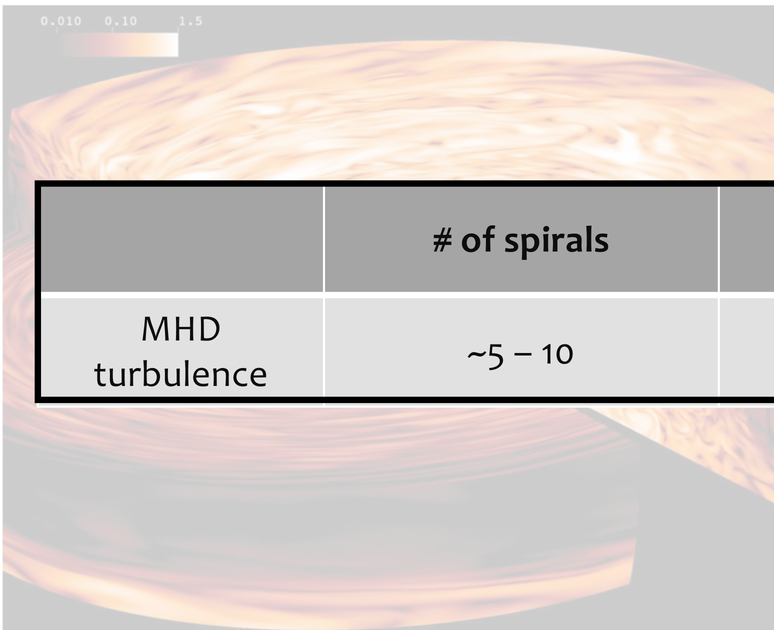

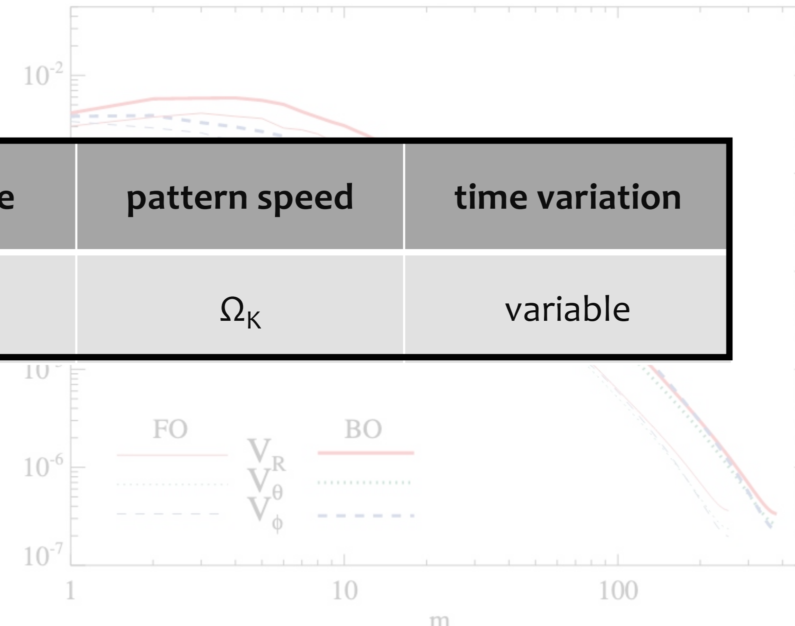

	# of spirals	pitch angle	pattern speed	time variation
MHD turbulence	~5 – 10	$\lesssim 10^\circ$	Ω_K	variable

Flock et al. (2011)

see also Heinemann & Papaloizou (2009), Suzuki & Inutsuka (2014), Gogichaishvili et al. (2017)

Spirals by infall

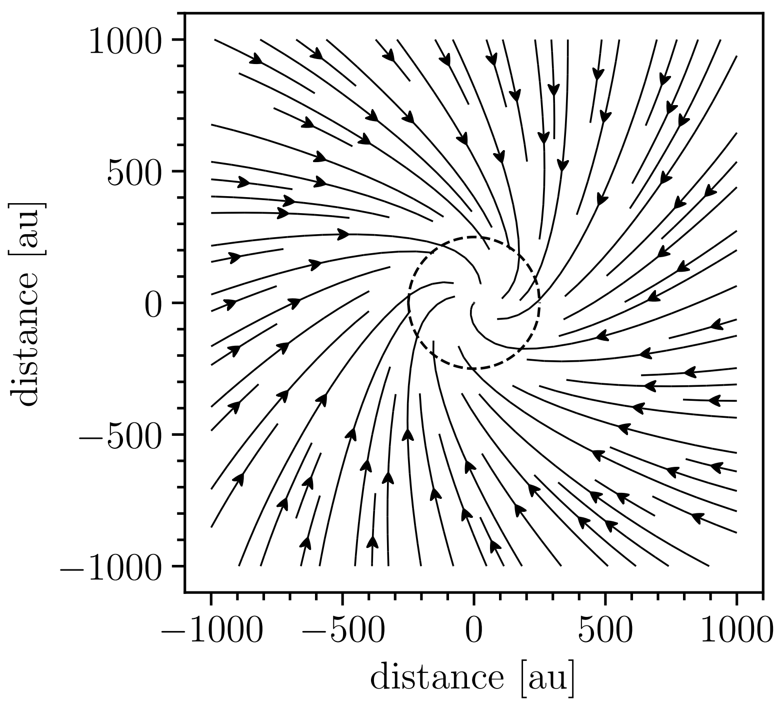

streamlines from the rotating isothermal cloud collapse model

Ulrich (1976), Cassen & Moosman (1981), Terebey et al. (1984)

centrifugal radius

The shear between the infalling materials and the disk gas triggers a Kelvin-Helmholtz-type instability, generating spirals.

Spirals by infall

left: AB Aur

(Boccaletti et al. 2020)

right: RU Lup

(Huang et al. 2020)

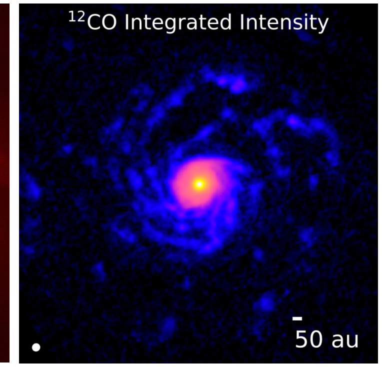

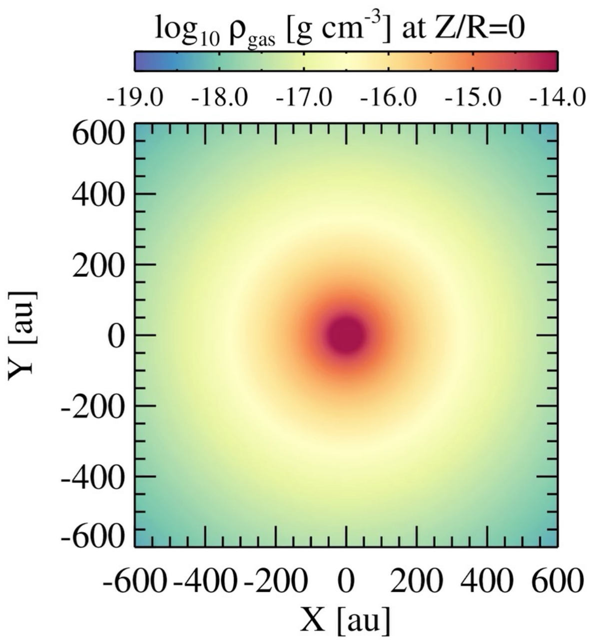

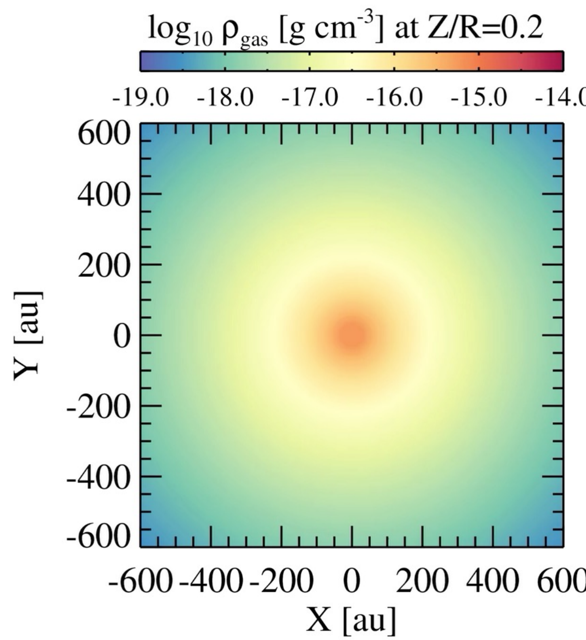

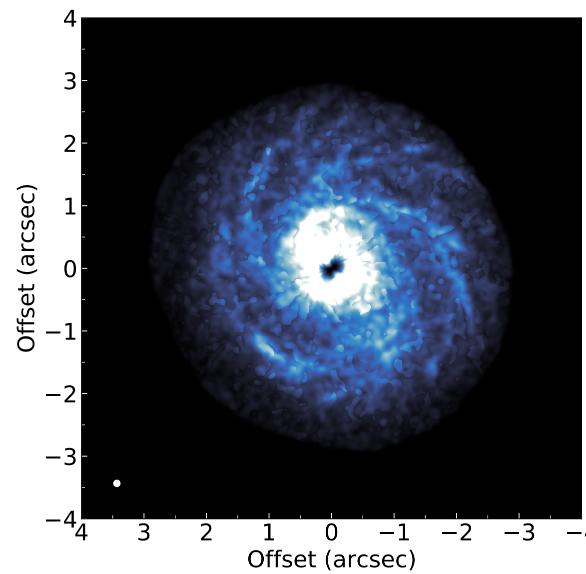

Bae et al. (in prep.)

see also Bae et al. (2015), Lesur et al. (2015), Hennebelle et al. (2016, 2017)

Spirals by infall

left: AB Aur

(Boccaletti et al. 2020)

right: RU Lup

(Huang et al. 2020)

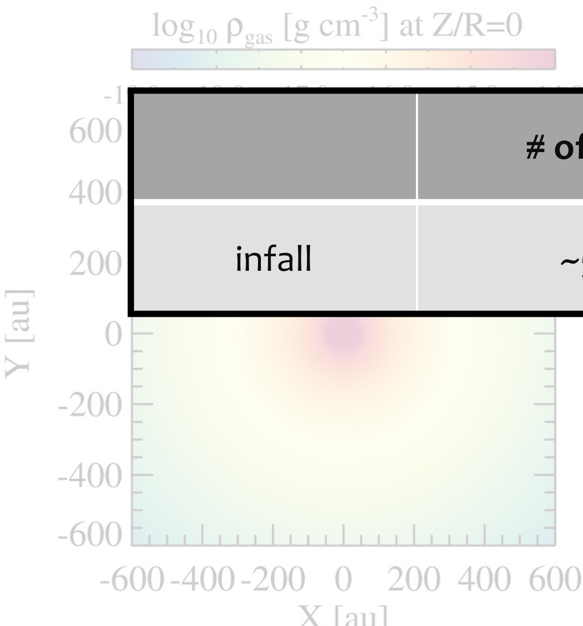

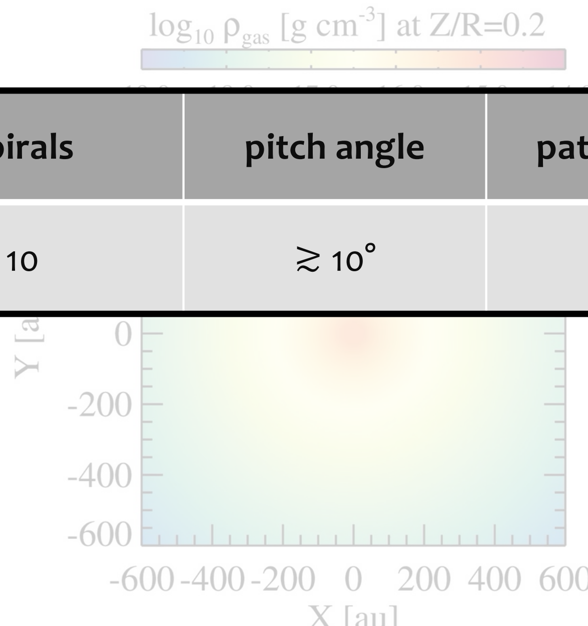

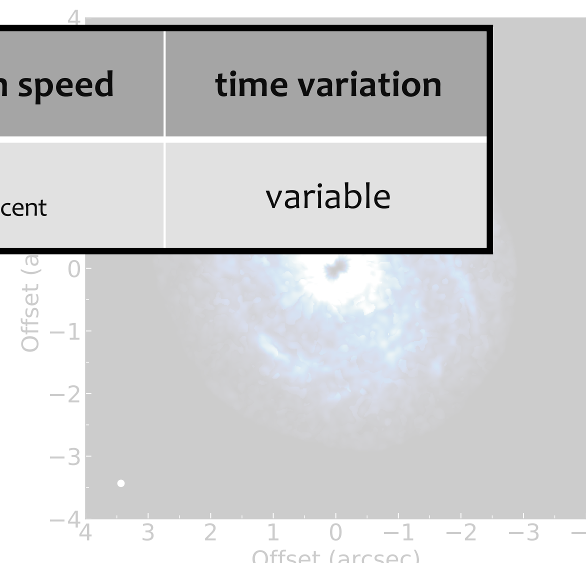

	# of spirals	pitch angle	pattern speed	time variation
infall	~5 – 10	$\gtrsim 10^\circ$	$\sim\Omega_{cent}$	variable

Bae et al. (in prep.)

see also Bae et al. (2015), Lesur et al. (2015), Hennebelle et al. (2016, 2017)

Spirals: summary

	# of spirals	pitch angle	pattern speed	time variation
companion (Lindblad)	2 – 3 in the inner disk 1 – 2 in the outer disk	~5° – 30°	Ω_c	steady
companion (buoyancy)	1 – a few	$\lesssim 10^\circ$	Ω_c	steady
stellar flyby	2	~10° – 30°	~Ω_c	disappear on the wave propagation timescale after the encounter
GI	2 – 10	~5° – 15°	Ω_K	variable
MHD turbulence	~5 – 10	$\lesssim 10^\circ$	Ω_K	variable
infall	~5 – 10	$\gtrsim 10^\circ$	~Ω_{cent}	variable

Rings: potential origins

- companion
- zonal flows
- inhomogeneous accretion
- icelines

	# of rings	ring location	ring width*	time variation
companion				
zonal flows				
inhomogeneous accretion				
icelines				

*The dust ring width can be much smaller than the gas ring width.

$w_d \simeq \left(\frac{\alpha}{St}\right)^{\frac{1}{2}} w_g$, where $St = \pi\rho_s s / 2\Sigma_g$

Rings: statistics

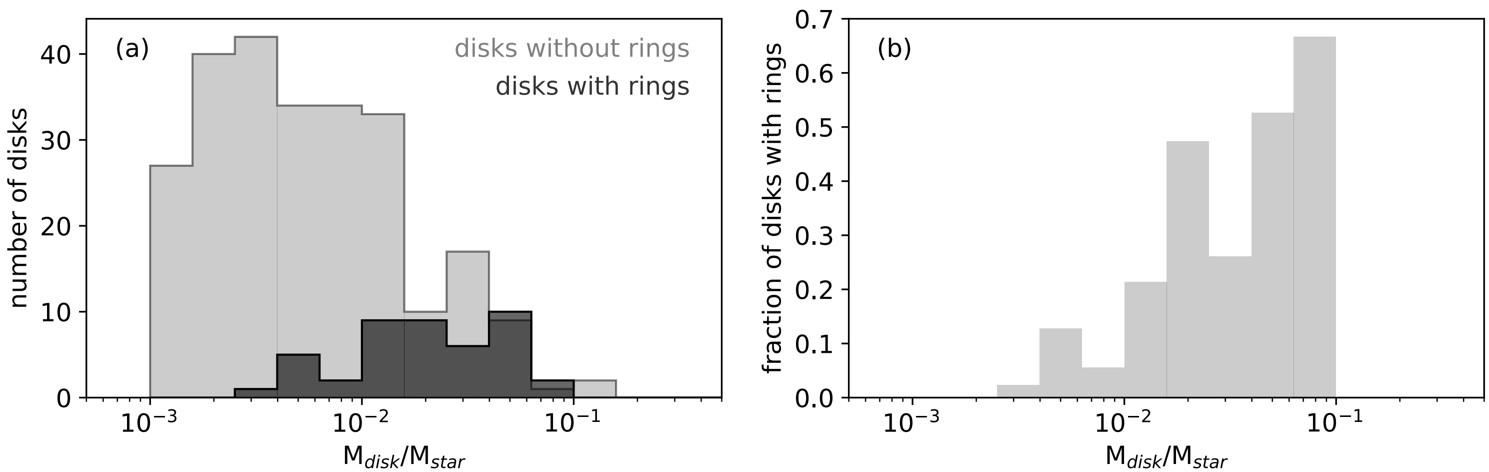

- Rings are detected in a larger fraction of massive disks ($M_{disk}/M_{star} \gtrsim 0.01$) compared with the low-mass counterpart.

Rings: statistics

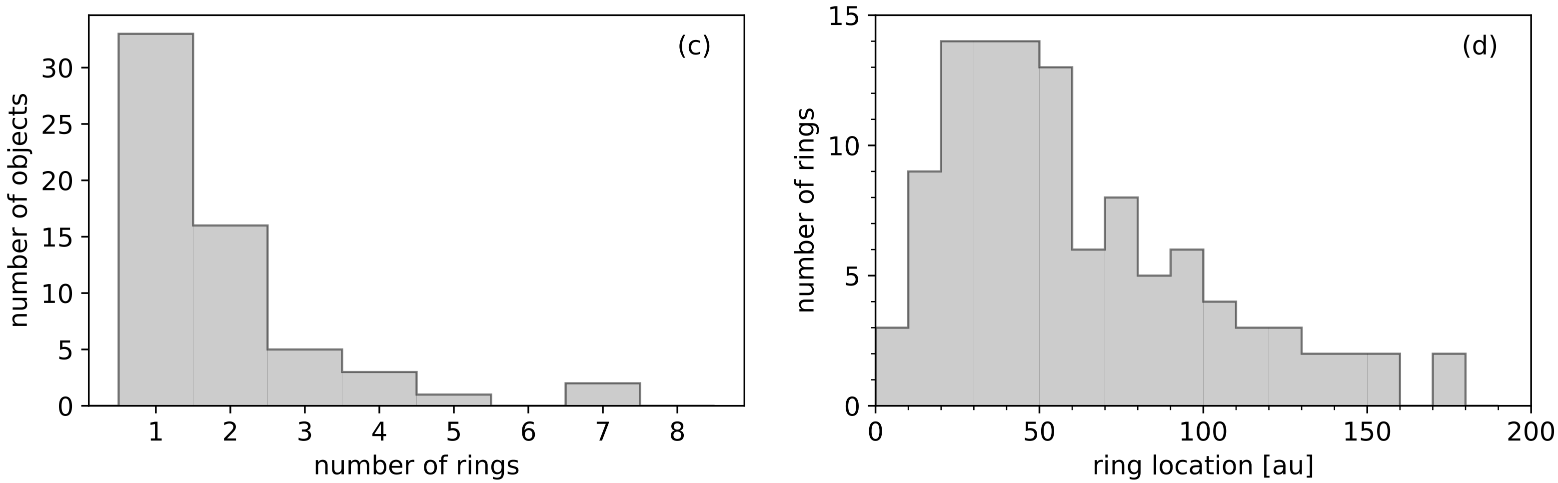

- Single- and double-ring systems are dominant (49/60).
- The number of rings decreases as a function of radial location.

Rings: statistics

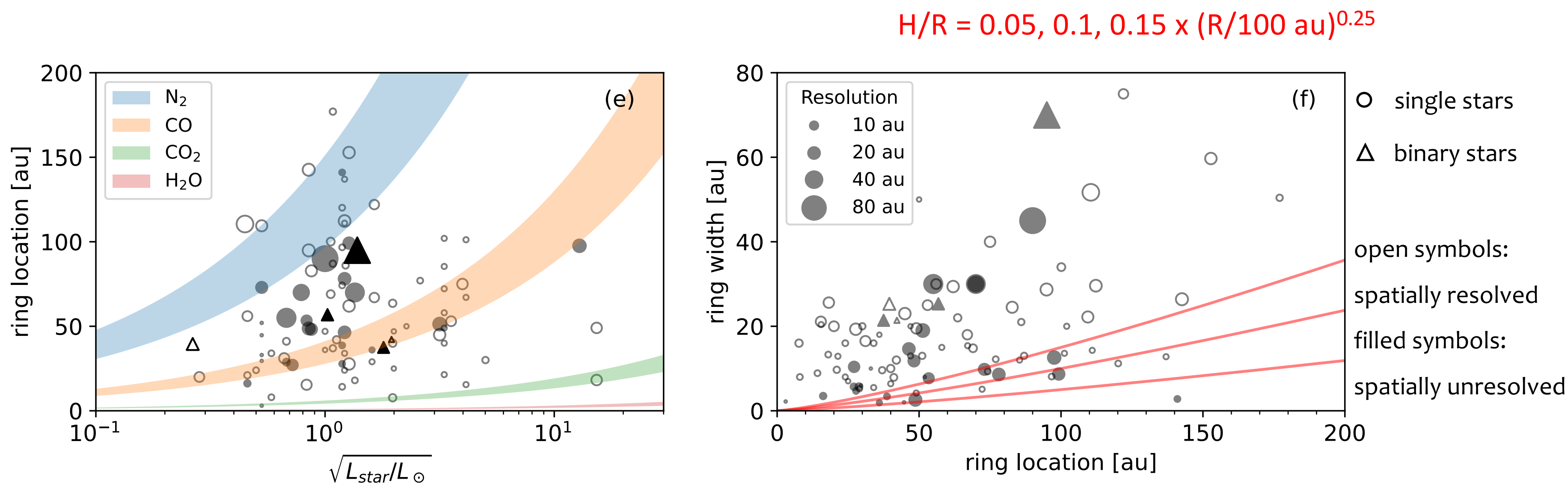

- No clear correlation is seen between the radial locations of the rings and the expected locations of icelines (see also Huang et al. 2018, Long et al. 2018, van der Marel et al. 2019).
- The width of most rings is greater than a gas scale height.

Rings by a companion

- Spiral arms transport angular momentum as they shock the disk gas, **opening gaps** (Goodman & Rafikov 2001, Rafikov 2002).

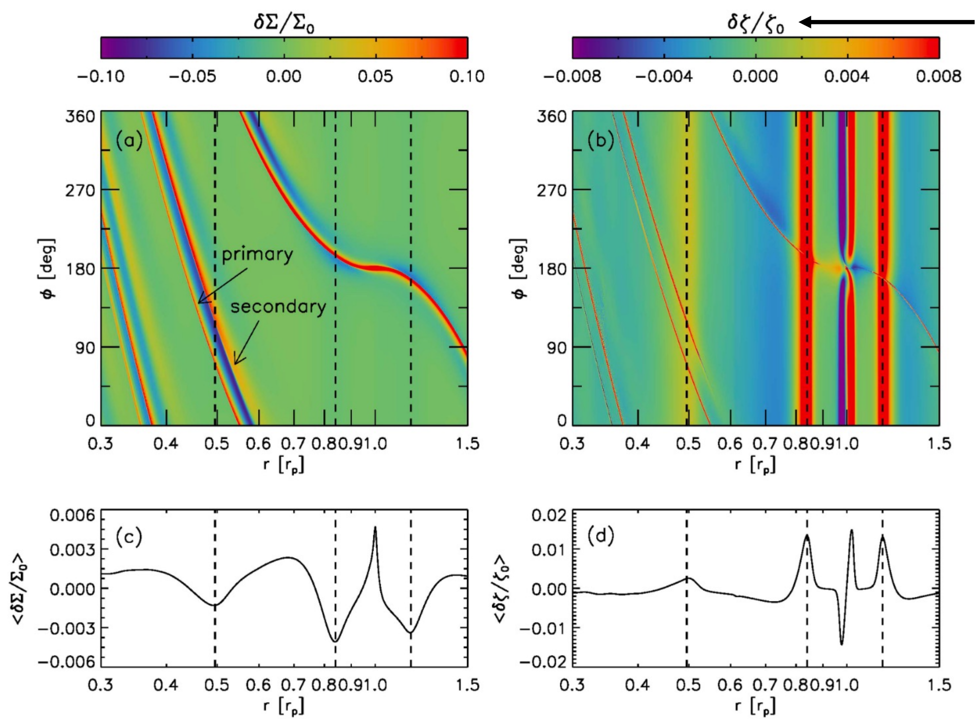

$$\zeta \equiv \frac{\nabla \times \boldsymbol{v}}{\Sigma}$$

potential vorticity: strictly conserved in the absence of shocks under a barotropic setup.

Bae et al. (2017)

Rings by a companion

- Spiral arms transport angular momentum as they shock the disk gas, **opening gaps** (Goodman & Rafikov 2001, Rafikov 2002).

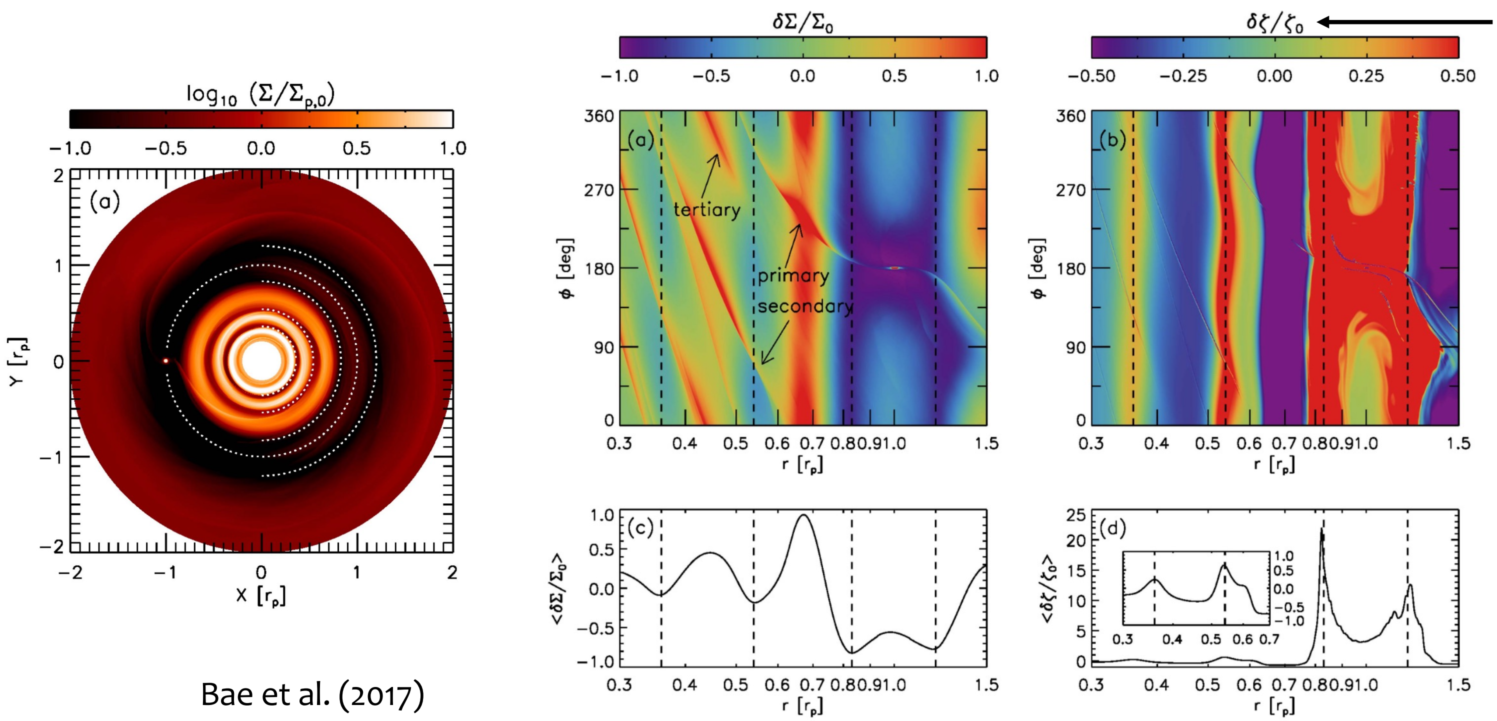

Bae et al. (2017)

$$\zeta \equiv \frac{\nabla \times \boldsymbol{v}}{\Sigma}$$

<u>potential vorticity</u>: strictly conserved in the absence of shocks under a barotropic setup.

Rings by a companion

- Thermodynamics matters.

Tc = β = cooling timescale/dynamical timescale

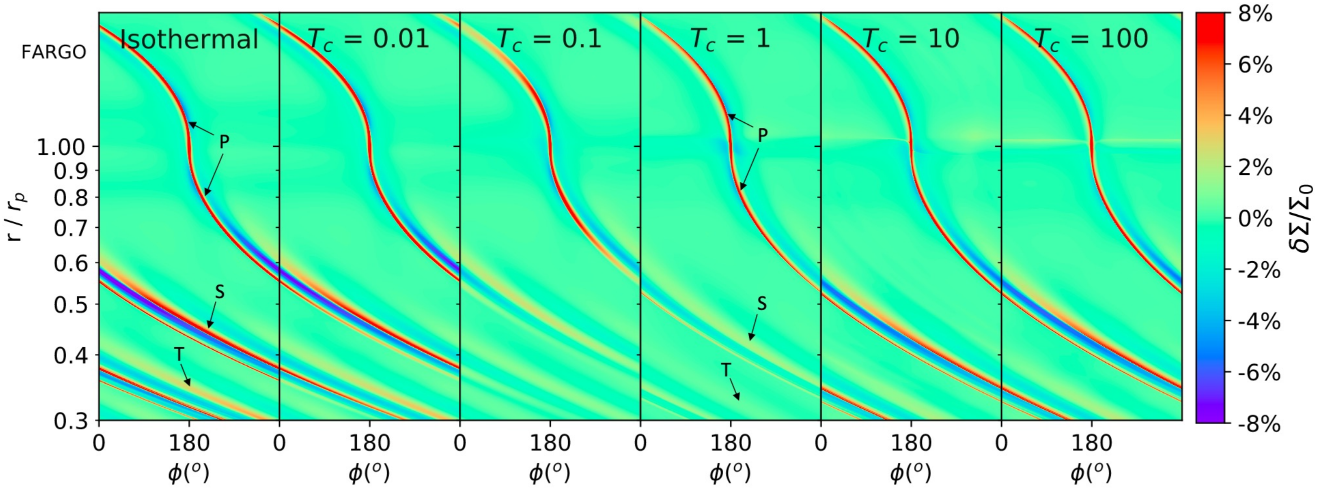

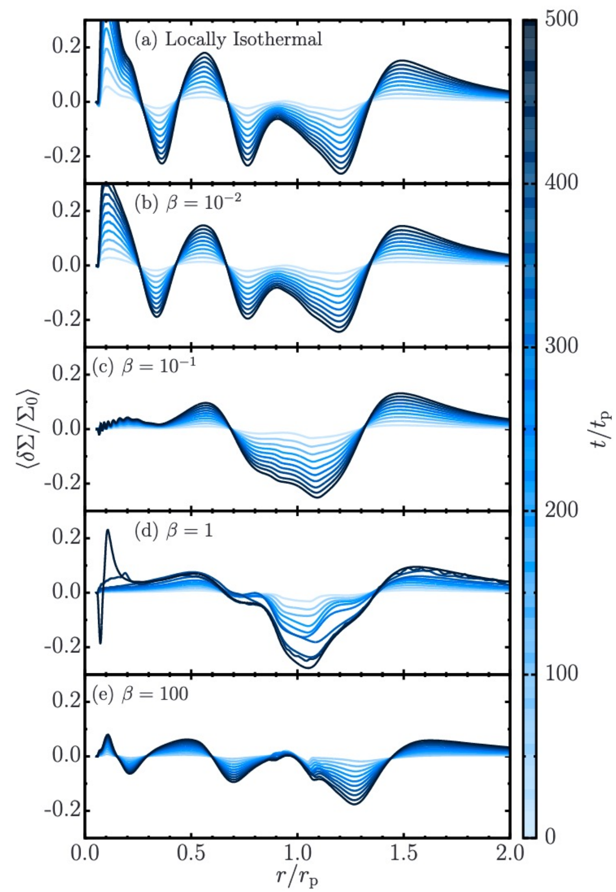

Left: Zhang & Zhu 2020, Right: Miranda & Rafikov 2020

Rings by a companion

- Thermodynamics matters.

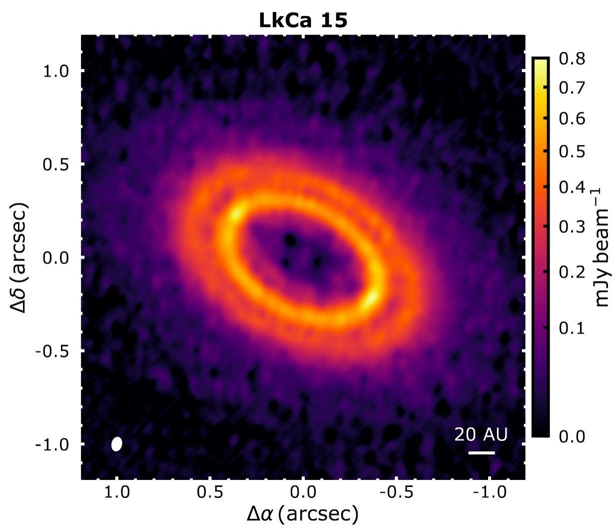

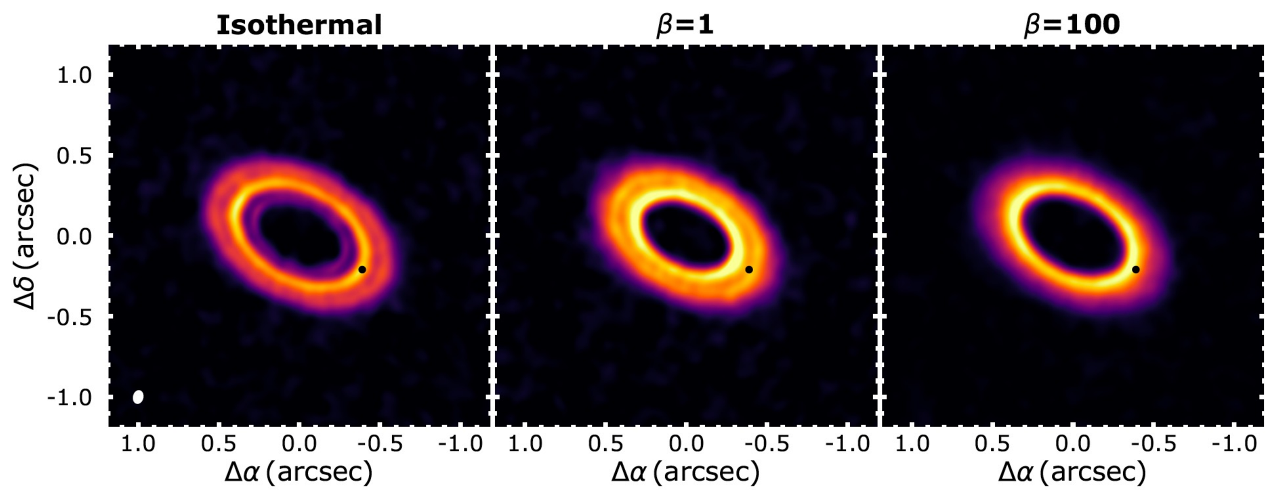

Facchini et al. (2020), see also Ziampras et al. (2020)

Rings by a companion

- Orbital migration can complicate things.

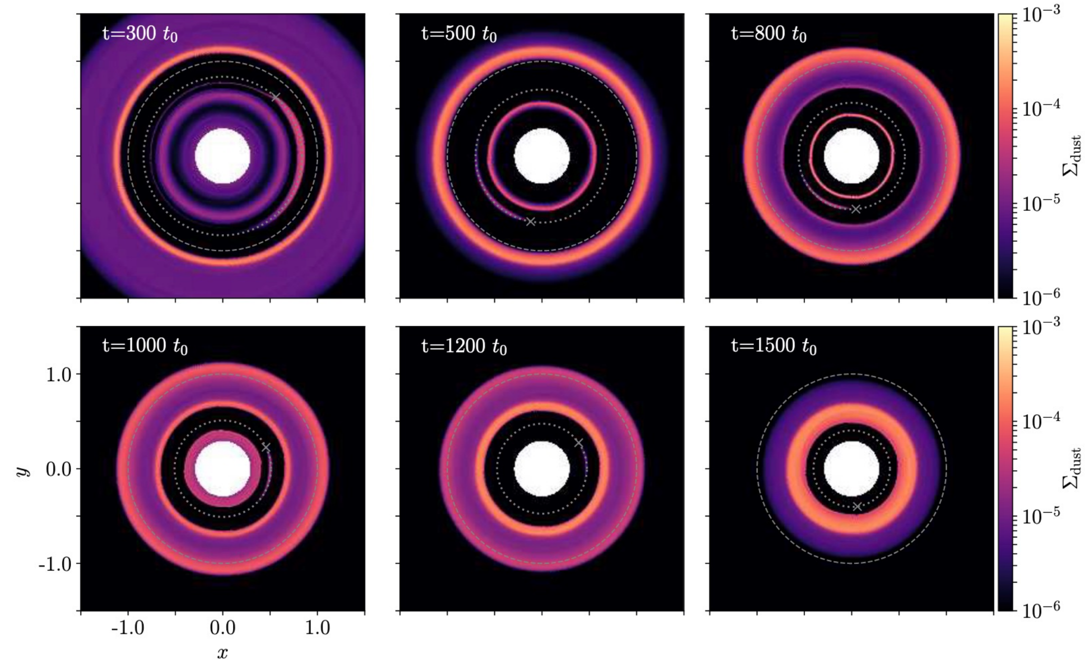

Kanagawa et al. (2021)

see also Meru et al. (2019), Nazari et al. (2019), Kanagawa et al. (2020), Wafflard-Fernandez & Baruteau (2020)

Rings by a companion

- Orbital migration can complicate things.

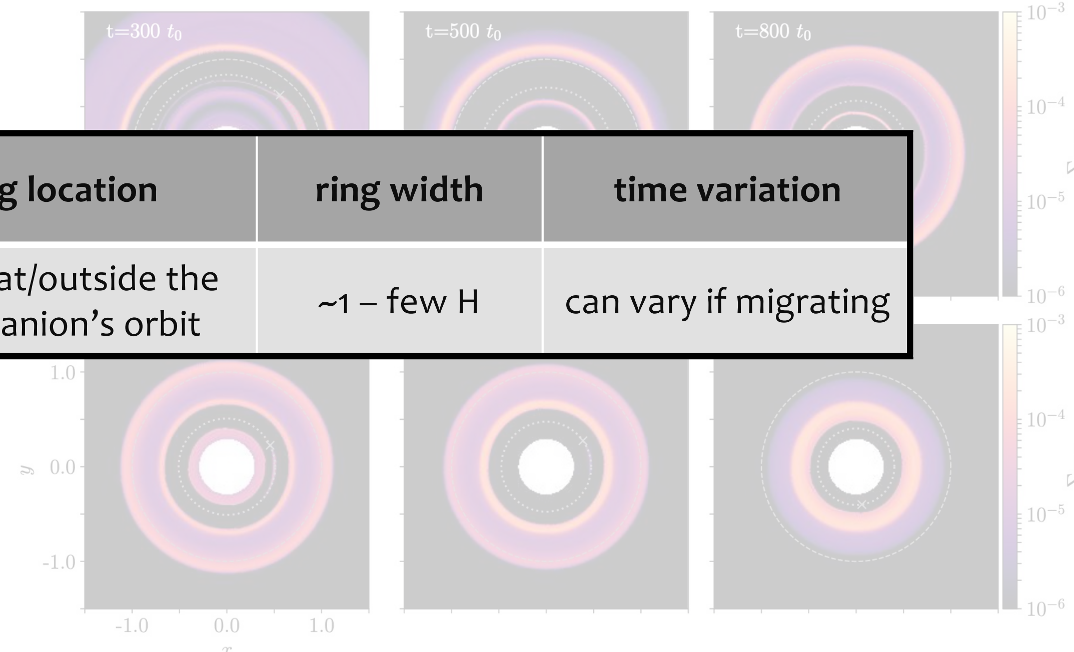

	# of rings	ring location	ring width	time variation
companion	1 – many	inside/at/outside the companion's orbit	~1 – few H	can vary if migrating

Kanagawa et al. (2021)

see also Meru et al. (2019), Nazari et al. (2019), Kanagawa et al. (2020), Wafflard-Fernandez & Baruteau (2020)

Rings by zonal flows – vertical shear instability

Pfeil & Klahr (2019)

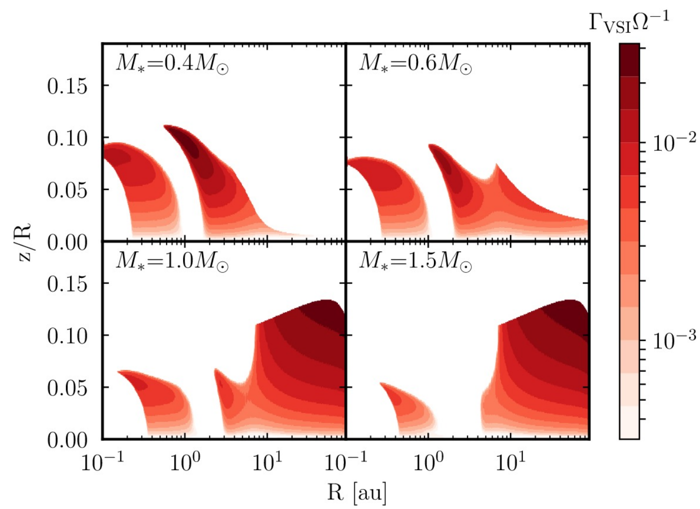

- Driven by the vertical "shear" in the rotational velocity.

$$\rho(R,\ Z) = \rho_0 \left(\frac{R}{R_0}\right)^p \exp\left(\frac{G\,M}{c_s^2}\left[\frac{1}{\sqrt{R^2+Z^2}} - \frac{1}{R}\right]\right),$$

$$\Omega(R,\ Z) = \Omega_K \left[(p+q)\left(\frac{H}{R}\right)^2 + (1+q) - \underline{\frac{qR}{\sqrt{R^2+Z^2}}}\right]^{1/2}$$

- Cooling requirement
  - Vertical shear is generally weak and can be stabilized by buoyancy if cooling is not efficient (Lin & Youdin 2015).
  - $t_{cool} \lesssim \frac{\left|\frac{r\partial\Omega}{\partial z}\right|}{N_z^2} \simeq \frac{h|q|}{\gamma-1}\Omega_K^{-1}$

Rings by zonal flows – vertical shear instability

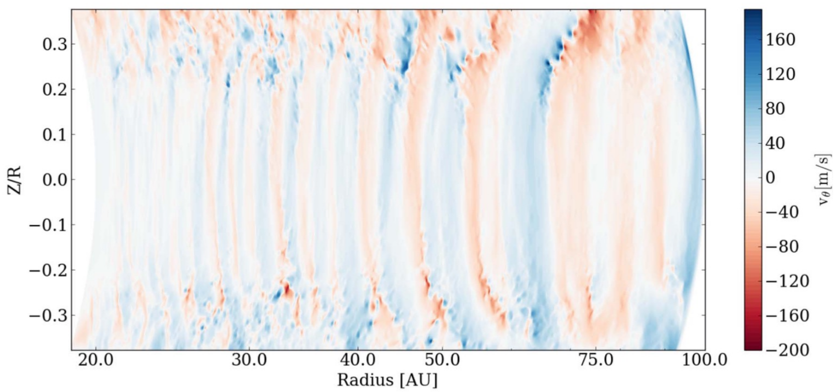

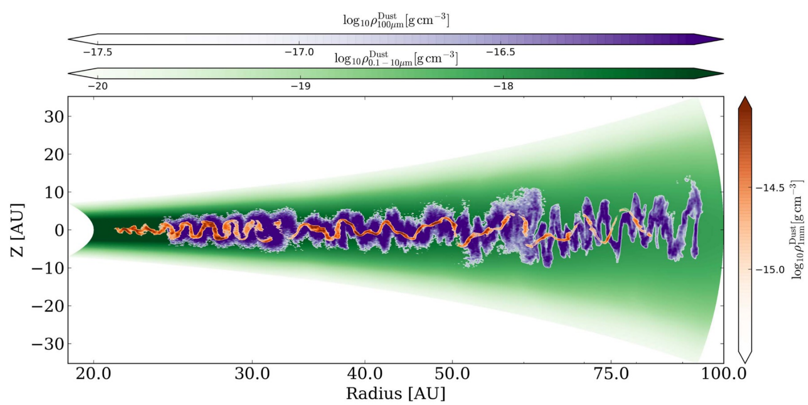

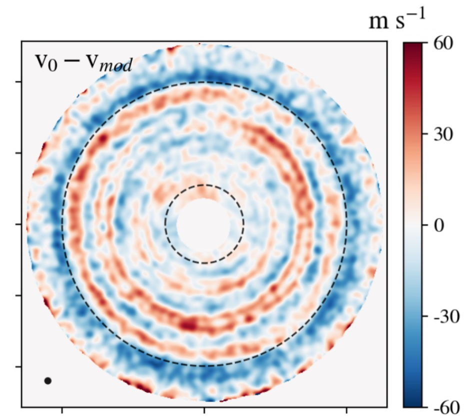

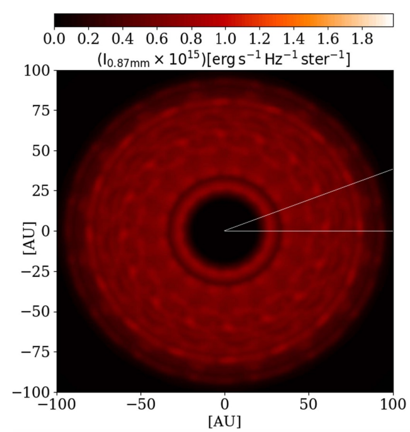

$k_r \simeq 5 – 20\ H^{-1}$

→ $\boldsymbol{\lambda}_r \simeq 0.3 – 1.2$ H

(Lin & Youdin 2015,

Pfeil & Klahr 2019)

Flock et al. (2017)
Barraza-Alfaro et al. (2021)

Rings by zonal flows – MHD

Typically multiple rings/gaps with widths of ~1 – 5 H

The properties depend on the magnetic field strengths/morphology

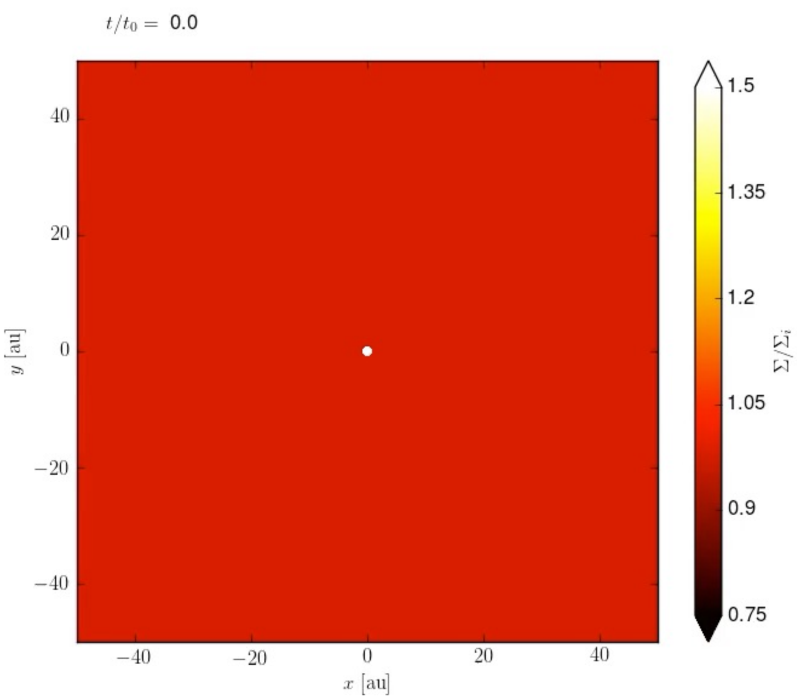

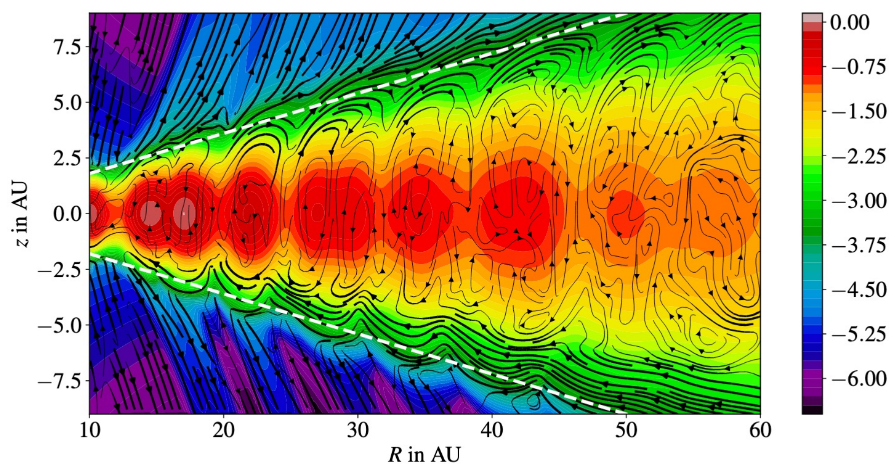

left: Suriano et al. (2019), right: Riols et al. (2020)

Rings by zonal flows – MHD

Typically multiple rings/gaps with widths of ~1 – 5 H

The properties depend on the magnetic field strengths/morphology

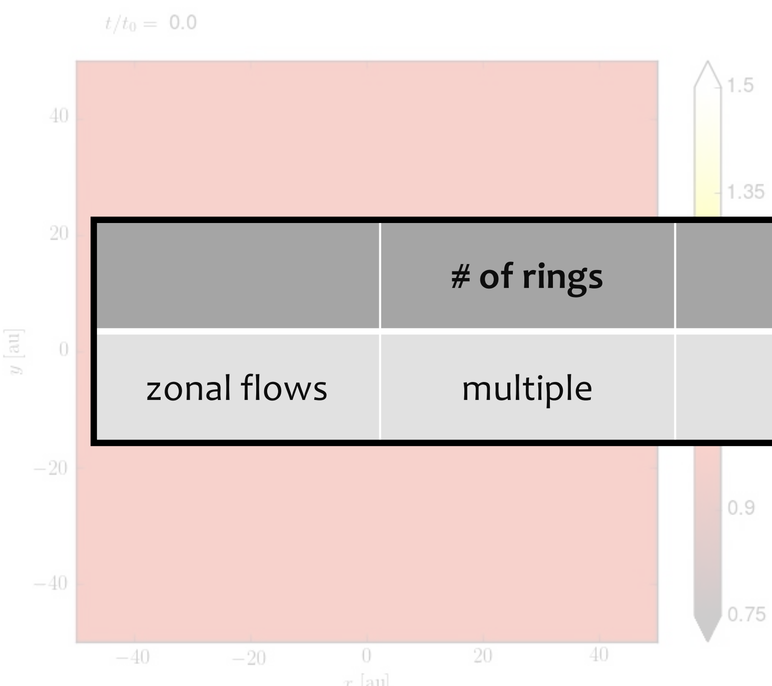

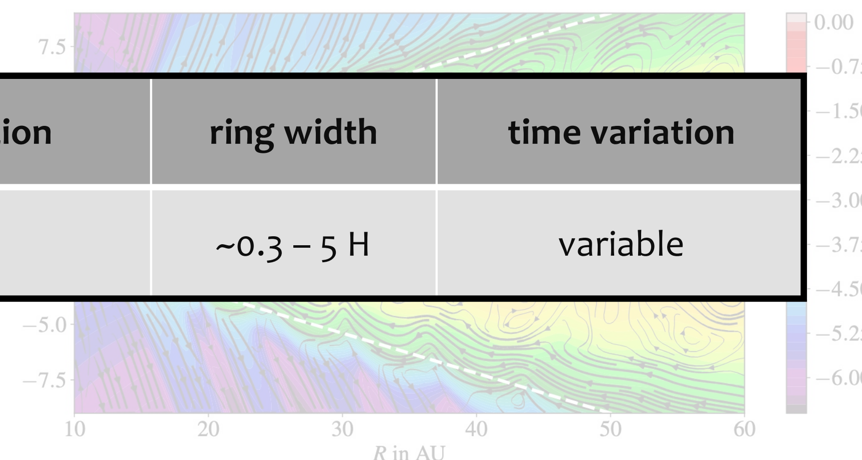

	# of rings	ring location	ring width	time variation
zonal flows	multiple	global	~0.3 – 5 H	variable

left: Suriano et al. (2019), right: Riols et al. (2020)

Rings by inhomogeneous accretion

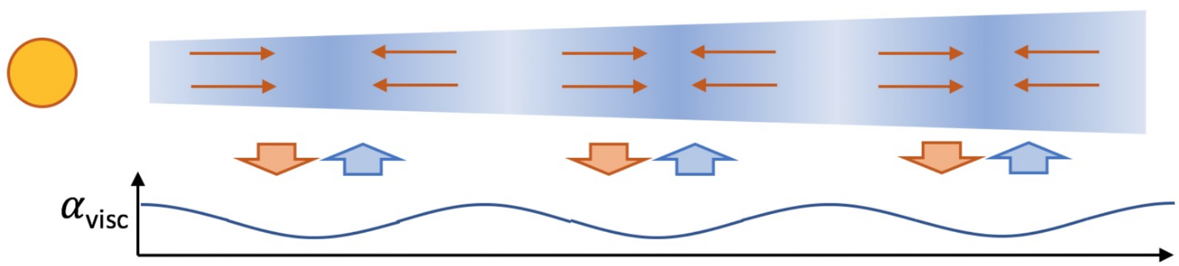

Perturbation in the gas (blue).

Dust (brown) drifts toward peaks of the perturbations.

This reduces the viscosity at those locations (brown arrow).

Thereby the gas perturbation is amplified (blue arrow).

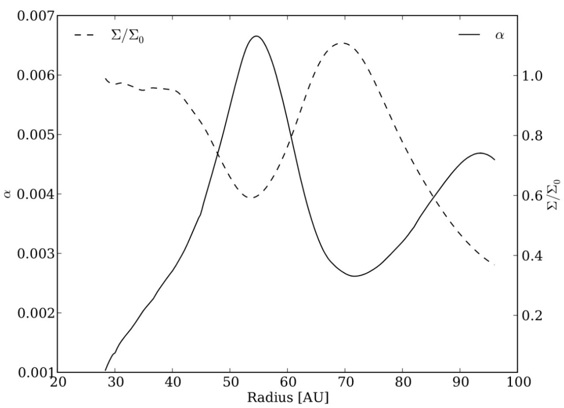

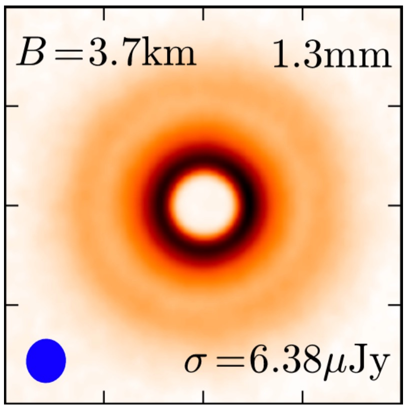

top: Dullemond & Penzlin (2018)

bottom: Flock et al. (2015)

Rings by inhomogeneous accretion

Perturbation in the gas (blue).

Dust (brown) drifts toward peaks of the perturbations.

This reduces the viscosity at those locations (brown arrow).

Thereby the gas perturbation is

	# of rings	ring location	ring width	time variation
inhomogeneous accretion	1 - many	low accretion	≳H	variable

top: Dullemond & Penzlin (2018)

bottom: Flock et al. (2015)

Rings by icelines

- grain size changes
- opacity changes across icelines
- radial drift speed changes
  - dust surface density changes
  - collisional growth/fragmentation rate changes
- sintering can enhance dust surface density
- ice “surfaces” instead of ice “lines”
- icelines can be thermally unstable

Ros & Johansen (2013), Schoonenberg & Ormel (2017), Drazkowske & Alibert (2017), Okuzumi et al. (2016), Sirono & Ueno (2017), Qi et al. (2019), Owen (2020), Tominaga et al. (2021)

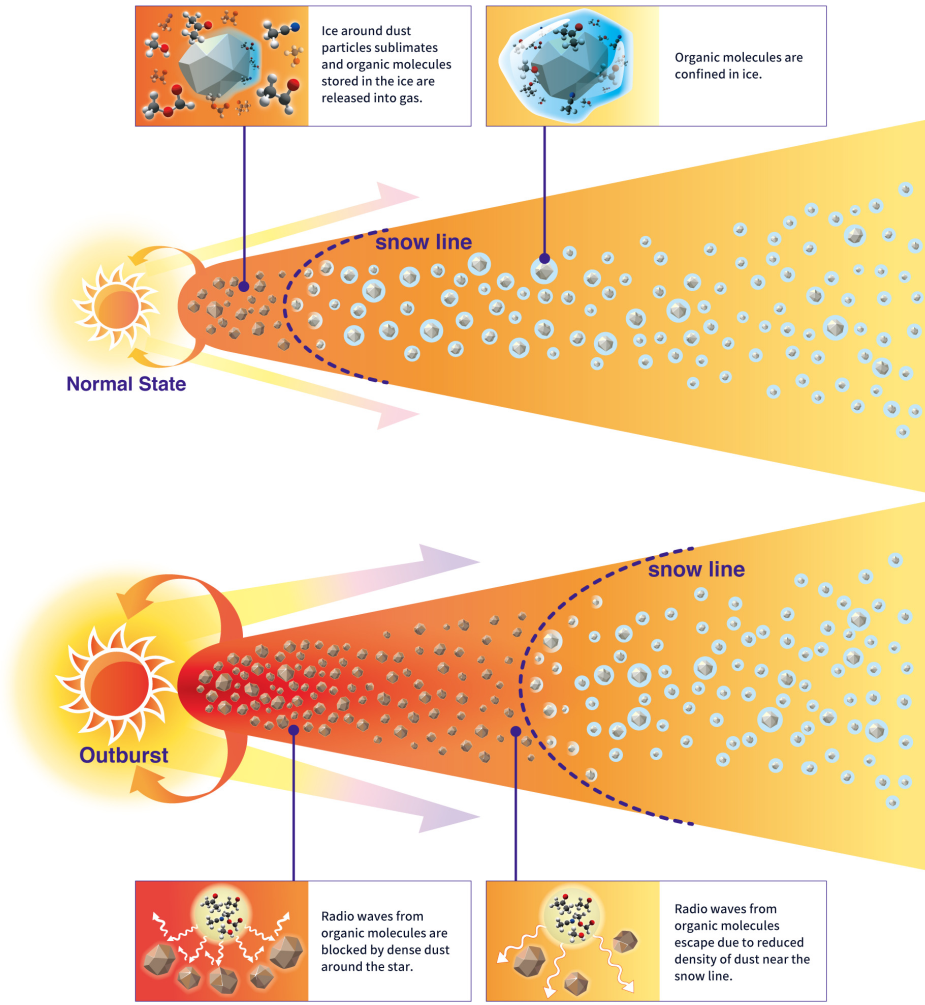

figure credit: Lee et al. (2019), NAOJ

Rings by icelines

- grain size changes
- opacity changes across icelines
- radial drift speed changes
- ice "surfaces" instead of ice "lines"
- icelines can be thermally unstable

	# of rings	ring location	ring width	time variation
icelines	~1 for species	inside/outside $T = T_{condensation}$	?	steady (but outburst, instability)

Ros & Johansen (2013), Schoonenberg & Ormel (2017), Drazkowske & Alibert (2017), Okuzumi et al. (2016), Sirono & Ueno (2017), Qi et al. (2019), Owen (2020), Tominaga et al. (2021)

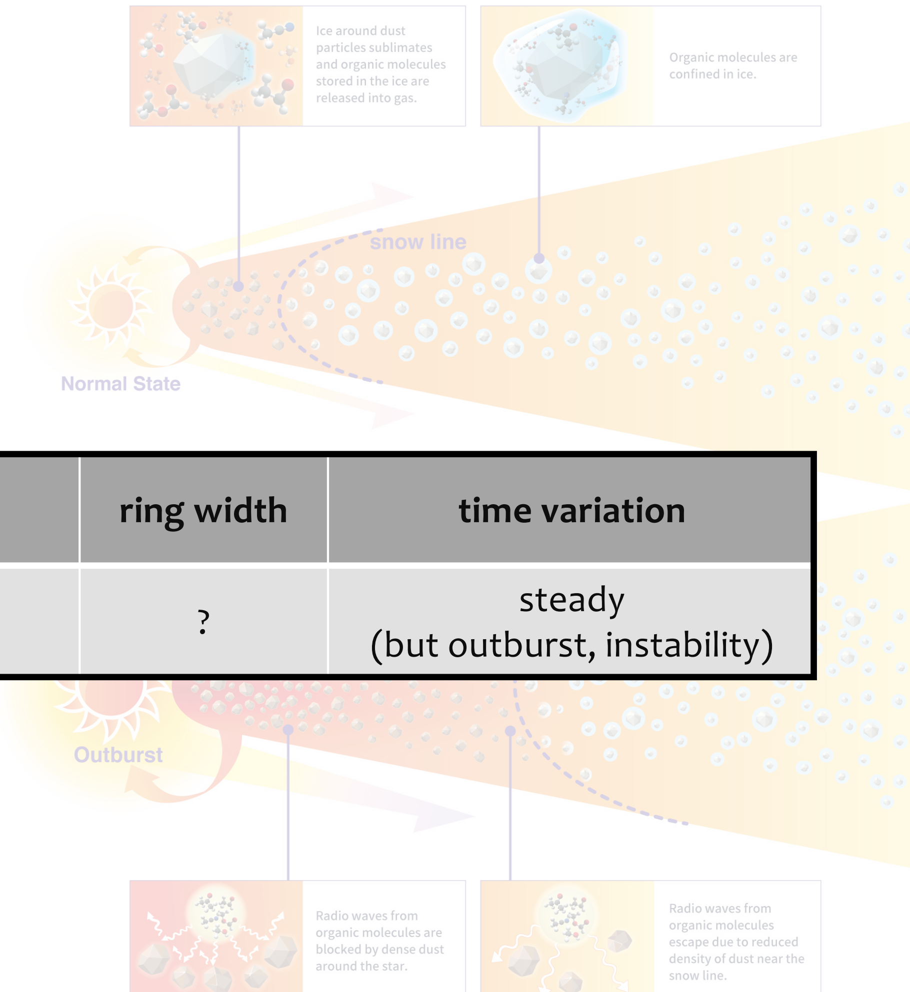

figure credit: Lee et al. (2019), NAOJ

Rings: summary

	# of rings	ring location	ring width	time variation
companion	1 – many	inside/at/outside the companion's orbit	~1 – few H	can vary if migrating
zonal flows	multiple	global	~0.3 – 5 H	variable
inhomogeneous accretion	1 - many	low accretion	$\gtrsim$H	variable
icelines	~1 for species	inside/outside $T = T_{condensation}$	?	steady (but outburst, instability)

Summary

- Disk substructures appear to be ubiquitous.
- Proper statistical studies would require homogeneous data sets and data analysis.
- Linking dust substructures to the underlying gas (sub)structure is often challenging.
- Numerical simulations do not always include both gas and dust.
- There are probably as many mechanisms as the number of disks with substructures.
- How can we possibly distinguish different possibilities?
  - I'd argue that we need to find the cause of substructures more directly.

Origin	Observable signatures, diagnostics	Required observations (aka theorists' wish list)
companion	direct detection (IR, Hα, CPD)	high angular resolution imaging
	kinematic planetary signatures	high angular + velocity resolution line observations
stellar flyby	detection of flyby stars	large FOV imaging, proper motion with Gaia
MHD	direct detection of magnetic fields	continuum/line polarization observations
zonal flows	coherent vertical motions for upper & lower surfaces	high angular + velocity resolution line observations
GI	large disk mass	measure surface density (how?) & temperature
	spiral pattern speed & pitch angle	long-term monitoring, high angular resolution imaging
infall	large-scale envelope, streamers	medium/low-resolution mosaic line observations
	shocks	shock tracers (e.g., SO), chemical tracers
inhomogeneous accretion	variable accretion rates inside/outside a ring	turbulence measurement using line observations (but what if accretion is not arising from turbulence?)
iceline	condensation temperature	temperature measurements for a large sample
	grain size changes across icelines	multi-wavelength continuum observations
dust backreaction	high dust-to-gas mass ratio	measure both gas and dust surface density (how?)